FMH606 Master's Thesis 2023
Process technology

Physicochemical properties (density and viscosity) of amine solvents for post-combustion CO₂ capture process

Ali Omidbeigi

Faculty of Technology, Natural sciences, and Maritime Sciences
Campus Porsgrunn

University of South-Eastern Norway

www.usn.no

Course: FMH606 Master's Thesis, 2023

Title: Physicochemical properties (density and viscosity) of amine solvents for post-combustion CO_2 capture process

Number of pages: 67

Keywords: Carbon capture processes, Physicochemical properties, Monoethanolamine (MEA), 2-amino-2-methyl-1-propanol (AMP), Redlich-Kister polynomial, Aronu, Hartono, and Svendsen equation (Aruno model), Eyring's viscosity model, Arrhenius equation.

Student:	Ali Omidbeigi
Supervisor:	Sumudu Karunarathne, Lars Erik Øi
External partner:	None

Summary:

Carbon capture technologies are becoming increasingly important as the negative effects of greenhouse gas emissions on the environment and human health become more evident. A key component of carbon capture processes is amine solvents, and understanding their physicochemical properties is crucial to improving the efficiency and effectiveness of carbon capture systems. By studying these properties, researchers can develop improved solvents that enhance carbon capture efficiency and optimize the design of carbon capture systems for specific industrial applications.

The focus of this work is to measure the density and viscosity of Monoethanolamine (MEA) and 2-amino-2-methyl-1-propanol (AMP). The experiments began by measuring the density of MEA and AMP at weight fractions from 0.3 up to 1 and a temperature range of 303.15 K up to 353.15 K using an Anton Paar DMA 4500 density meter. The viscosity was measured at same weight fractions and temperature range using an Anton Paar MCR 101 rheometer and compared with relevant literature resources.

The results of the density measurements for MEA were compared with two relevant previous works, revealing an average absolute relative deviation (AARD) and absolute maximum deviation (AMD) between all the data of this work and data from both sources of 0.03% and 0.284 kg/m^3 AMD in comparison with one source and 0.03% and 0.2843 kg/m^3 with the other. The results of AMP could be compared with only one previous work due to the lack of available articles for this amine, and the AARD and AMD were found to be 0.22% and 9.2 kg/m^3 , respectively.

Mathematical models were developed for each set of measurements. For density, Redlich-Kister polynomial and Aronu, Hartono, and Svendsen equation (Aruno model) were suggested. The fitted curves and calculations showed an AARD of 0.05% and AMD of 2.85 kg/m^3 for aqueous MEA using the Redlich-Kister model, while the Aruno model values were found to be 0.02% and 5.46 kg/m^3. For aqueous AMP, the Redlich-Kister model showed 0.16% AARD and 10.55 kg/m^3 AMD, and the Aruno model had 0.12% AARD and 9.24 kg/m^3 AMD.

In viscosity modeling, Eyring's viscosity model and Arrhenius equation were investigated. In both cases of MEA and AMP solutions, the Arrhenius equation showed more satisfactory results, with an AARD of 9.86% for MEA and 3.76% for AMP. The AMD values were 1.94 mPa.s and 4.28 mPa.s, respectively.

At the final step, this study suggests expanding experimental investigations and advancing mathematical modeling for future work. Some weak points identified and to address these issues, the study includes recommendations such as, investigating properties of mixtures of AMP and MEA, studying CO_2 loaded AMP solutions, and evaluating other well-known viscosity and density models.

Preface

The world is facing unprecedented challenges in terms of climate change and the impact of human activities on the environment. Carbon capture processes are gaining more attention as one of the possible solutions to moderate the harmful effects of greenhouse gases on the planet. In this context, the Physicochemical properties of amine solvents used in post-combustion CO_2 capture processes play a critical role in improving the efficiency and effectiveness of such processes.

This master thesis article was offered by the University of South East Norway for process technology students. The title of the thesis, "Measurement of Physicochemical Properties of Amines for Post-Combustion CO_2 Capture Processes," caught my attention as it involved both laboratory work and mathematical simulations. Moreover, the research topic was aligned with my previous group project, which further motivated me to delve deeper into this field.

After consulting with our course instructors, who are among the pioneers in this field, Monoethanolamine (MEA) and 2-amino-2-methyl-1-propanol (AMP) were chosen for experimentation. The aim of this work was to measure the density and viscosity of these amines at different weight fractions and temperature ranges and compare the results with existing literature. Additionally, mathematical correlations were developed to provide better data for designing and calculating processes related to carbon capture.

I would like to express my sincere gratitude to Sumudu Karunarathne and Lars Erik Øi, who provided invaluable training and intellectual support throughout this project. Their flexibility in accommodating my schedule was also greatly appreciated.

Porsgrunn, 30 April 30, 2023

Ali Omidbeigi

Contents

Nomenclature

Symbol	Definition	Unit
MEA	Monoethanolamine	-
AMP	2-amino-2-methyl-1-propanol	-
CO_2	Carbon dioxide	-
M	Molar weight	$g/mole$
v	Molar volume	$m^3/mole$
x_i	Mole fraction of component i	-
w_i	Mass ratio of component i	-
R^2	R-squared	-
ΔG	Free energy of activation for viscous flow	J/mol
R	Universal gas constant	$\dfrac{J}{mol.K}$
h	Planks constant	m^2kg/s
N_A	Avogadro's number	m^2kg/s
AARD	Average absolute relative deviation	-
AMD	Absolute maximum deviation	-

1 Introduction

Post-combustion capture is a method of capturing CO_2 from flue gases produced by burning fossil fuels and biomass in air. Rather than being released directly into the atmosphere, flue gas is routed through equipment designed to isolate the majority of the CO_2. The captured CO_2 is then transferred to a storage reservoir while the remaining flue gas is discharged into the atmosphere. Various techniques have already been developed for CO_2 capture techniques such as Solvent (absorption), membranes, solid sorbents, and cryogenic, however separation by chemical absorbent which its process flow diagram is illustrated in figure 1.1 is the most widely implemented method [1].
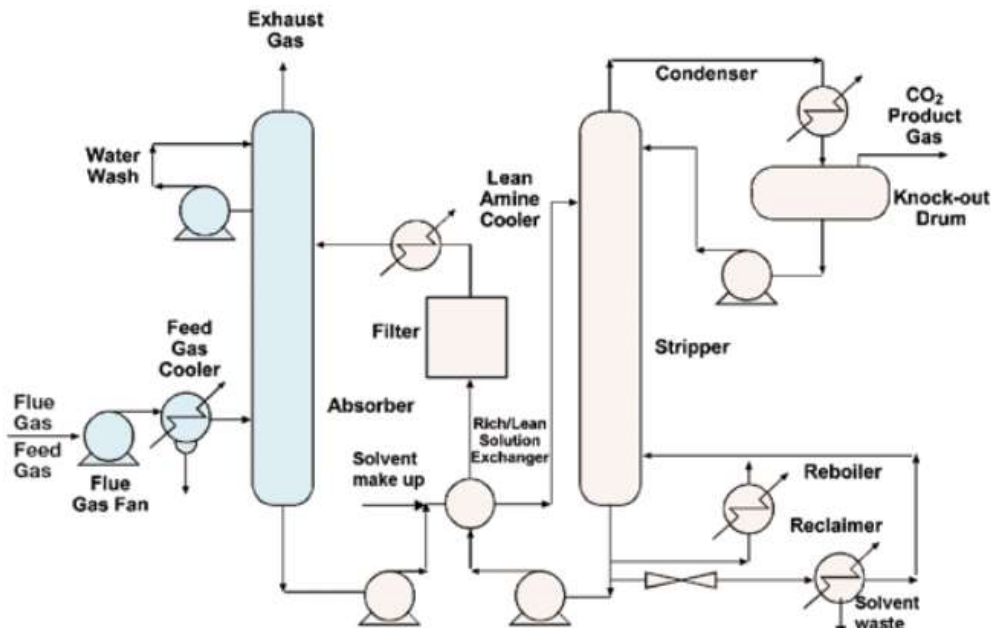
Figure 1.1: Process flow diagram for CO2 recovery from flue gas by chemical absorption [1].

By diverting the focus on the chemical absorption process, the importance of knowing the physicochemical properties such as density and viscosity continues to increase.

Mass transfer coefficients like Chilton-Colburn factor, Sherwood number, and Reynolds number play a key role in designing an absorption system like packed towers since it can determine major details such as absorption capacity as well as dimensional characteristics of the system by describing significant numbers like number of transfer units (NTU) and height of transfer units (HTU) resulting in sizing towers [2].

Density and viscosity of the solvent has powerful influence on calculating the mass transfer coefficients. As it revealed during this work and confirmed by literature resources, The density of the amine solvent increases with increasing amine concentration and decreases with increasing temperature. Therefore, the solvent's density changes during the absorption and regeneration processes hence, the relationship between the density of the solvent concentration, and temperature is crucial for predicting the performance of the CO_2 capture process.

Viscosity is another essential property of amine solvents for CO_2 capture. The viscosity of the solvent like the density, influences the calculations. The viscosity of amine solvents generally increases with increasing amine concentration and decreases with increasing temperature.

In summary, accurate measurements and understanding of physicochemical properties are essential for developing reliable models and optimizing the process. In this study, the main objective was to measure the viscosity and density of two types of amines at varying mole fractions and temperatures.

The results of these measurements are subsequently tabulated and compared with existing literature data to evaluate their accuracy. Furthermore, some mathematical correlations are developed based on the findings and their accuracy and reliability are assessed.

By conducting these measurements and developing reliable correlations, it contributes to a better understanding of the physicochemical properties of amine solvents and facilitate the development of more effective post-combustion CO_2 capture processes.

1.1 Background

Numerous studies have been conducted on amines physicochemical properties since the early commercial-scale projects of carbon capture developed. Sleipner project commissioned during 1996 in Norway, may be the initial point for industrial application of those studies [1].

Commonly investigated amines in industry are Monoethanolamine (MEA), Diethanolamine (DEA), Piperazine, Diethylenetriamine (DETA), Methyl diethanolamine (MDEA), Ethanolamine (ETA), Diglycolamine (DGA), and 2-amino-2-methyl-1-propanol (AMP) Each amine has different properties and is selected based on factors such as the operating conditions and the specific goals of the carbon capture project [3], [4]. In addition to aqueous amine solutions sometimes hybrid or mixed amines are implemented as Cheng-Hsiu Yu et al. mentioned "*Because of various properties and advantages of various amines, mixed amines have been proposed to enhance CO₂ capture efficiency and to reduce regeneration cost [3].*"

As mentioned above, choosing an absorbent for carbon capture depends on various variables which this work is not covering those variables, but as a general overview, advantages and disadvantages of some of the organic sorbents are summarizes in table 1.1.

Table 1.1: Brief comparison between most common amines [3].

Amine name	Advantage	disadvantage
MEA	Prompt reaction with CO_2	High energy demand in regeneration
MDEA	High absorption capability Low regeneration energy demand	Slow reaction
DEA	Prompt reaction with CO_2	High energy demand in regeneration
AMP	High absorption capability	High material price
Piperazine	High absorption capability	High material price Toxicity and corrosion effects

1.2 Work criteria selection

Undoubtedly determining the area of focus is crucial for experimental studies like the current work. In this work the aim is to measure density and viscosity of organic sorbents (amins) implemented in post-combustion carbon capture process and since the Physicochemical properties are predetermined, the type of amine is left to specify.

For this work, aqueous MEA and aqueous AMP are chosen for the experiments for following reasons.

> ➢ Monoethanolamine (MEA) is considered as the most extensively used amine in the carbon capture process due to its effective carbon dioxide (CO_2) absorption capacity. As a result, numerous reliable data are available that can be utilized to compare the accuracy of experimental outcomes and mathematical models.
> ➢ The limited number of available studies on aqueous AMP (2-amino-2-methyl-1-propanol) represents a significant gap in the literature and presents a promising area for future research. The lack of information on this topic suggests that working on aqueous AMP has the potential to yield valuable insights and contribute to the current understanding of its properties and behavior in various applications.

To ensure consistency with previous research, weight fractions ranging from 0.3 to 1 were selected for both amines, as this range is commonly used in reporting findings in the field.

2 Previous works and study

This section of the report will focus on reviewing relevant data and research on AMP and MEA. Due to the extensive use of MEA in various applications, a wealth of reliable data is readily available. For the purposes of this investigation, the most recent and relevant research papers on MEA will be reviewed. Conversely, as AMP is not as commonly used as an absorbent, the availability of data on this particular compound is limited.

2.1 Aqueous MEA previous work and study

Due to the number of studies done on Monoethanolamine and its various combinations with other amines, a substantial source of scholarly literature is currently available for comparative analysis with the present research findings.

The research conducted by Karunarathne et al. [5] and Trine et al. [6] have been utilized for comparisons and data validation purposes of MEA density and viscosity. The findings of their work have been included in Table 2.1, with Karunarathne et al.'s research covering density data for aqueous MEA at temperatures ranging from 30℃ to 80℃, and Trine et al.'s research covering measurements from 30℃ to 80℃. Both studies have used the same weight fractions of MEA/H_2O (w_1), ranging from 0.3 to 1.

It is worth noticing that Trine et al. conducted their measurements using a Viscometer (Z1DIN), whereas Karunarathne et al. used an Anton Paar MCR 101 rheometer. However, both studies utilized a DMA 4500 Anton Paar density meter for their density measurements [6],[5].

Table 2.1: Density (ρ) of aqueous MEA at different temperatures and wight fractions reported by Karunarathne et al. and Trine et al. [5], [6].

T (℃)		w_1							
		0.3	0.4	0.5	0.6	0.7	0.8	0.9	1
		$\rho\ (g/cm^3)$							
30	Source 1	N.A.	N.A.	N.A.	N.A.	N.A.	N.A.	N.A.	N.A.
	Source 2	1.0082	1.0133	1.0178	1.0212	1.0224	1.0208	1.0158	1.0081
40	Source 1	1.0034	1.0077	1.0117	N.A.	1.0155	N.A.	1.0084	1.0003
	Source 2	1.0033	1.0078	1.0116	1.0145	1.0152	1.0133	1.0081	1.0001
50	Source 1	0.9981	1.0018	1.0053	N.A.	1.0082	N.A.	1.0006	0.9923
	Source 2	0.9979	1.0018	1.0052	1.0076	1.0079	1.0057	1.0003	0.9921
60	Source 1	N.A.	N.A.	N.A.	N.A.	N.A.	N.A.	N.A.	N.A.
	Source 2	0.9916	0.9955	0.9984	1.0004	1.0004	0.9979	0.9924	0.984
70	Source 1	0.9858	0.9889	0.9915	N.A.	0.9930	N.A.	0.9846	0.9760
	Source 2	0.986	0.9889	0.9914	0.993	0.9927	0.99	0.9843	0.9759
80	Source 1	0.9794	0.9819	0.9842	N.A.	0.9850	N.A.	0.9764	0.9678
	Source 2	0.9794	0.9819	0.9841	0.9854	0.9848	0.9819	0.9761	0.9676

a) Trine et al.
b) Karunarathne et al.

The viscosity measurements of the aforementioned resources have been reported under identical conditions and are presented in Table 2.2.

Table 2.2: Viscosity (η) of aqueous MEA at different temperatures and wight fractions reported by Karunarathne et al. and Trine et al. [5], [6].

T (℃)		w_1							
		0.3	0.4	0.5	0.6	0.7	0.8	0.9	1
		$\eta\ (mPa.s)$							
30	Source 1	N.A.	N.A.	N.A.	N.A.	N.A.	N.A.	N.A.	N.A.
	Source 2	2.109	3.15	4.58	6.769	9.823	12.84	14.963	14.748
40	Source 1	1.67	2.28	3.39	N.A.	6.96	N.A.	10.20	9.61
	Source 2	1.628	2.3964	3.31	4.736	6.664	8.534	9.879	10.108
50	Source 1	1.33	1.75	2.54	N.A.	4.94	N.A.	7.06	6.72
	Source 2	1.29	2.002	2.454	3.444	4.72	5.937	6.829	6.935
60	Source 1	N.A.	N.A.	N.A.	N.A.	N.A.	N.A.	N.A.	N.A.
	Source 2	1.046	1.8776	1.915	2.602	3.461	4.295	4.936	5.067
70	Source 1	0.92	1.14	1.57	N.A.	2.79	N.A.	3.81	3.69
	Source 2	0.866	1.499	1.528	2.031	2.615	3.217	3.683	3.834
80	Source 1	0.77	0.95	1.28	N.A.	2.18	N.A.	2.93	2.85
	Source 2	0.74	1.2023	1.243	1.62	2.029	2.483	2.832	2.974

a) Trine et al.
b) Karunarathne et al.

2.2 Aqueous AMP previous work and study

Only limited literature data is available for the properties of 2-amino-2-methyl-1-propanol (AMP) with water. However, previous research has extensively investigated the properties of AMP mixtures with other amines, which are not directly relevant to this work. Henni et al. conducted one notable study in this area, and Table 2.3 summarizes their reported values for aqueous AMP density at various temperatures and mole fractions(x_1).

0.2939	22.7	16.96	12.51	7.85	5.23	3.67
0.4075	51.5	36.9	20.37	12.17	7.63	4.94
0.4982	76.8	54.3	28.7	16.26	10.00	6.43
0.5996	102.5	70.3	36.1	20.0	11.97	7.50
0.7028	124.3	84.0	42.5	22.7	13.33	8.23
0.8016	140.7	94.0	46.2	24.6	14.22	8.88
0.9001	149.1	98.9	47.9	25.3	14.53	8.98
1.0000	N.A.	N.A.	47.8	25.1	14.40	8.91

It is worth mentioning that Henni et al. conducted their experiment on viscosity using a Cannon-Ubbelohde viscometer and measured the density using a DMA 4500 Anton Paar density meter.
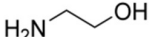
3 Chemicals and instruments

In this chapter, an overview will be provided of the chemical components used in the experiments, including their properties, sources, and preparation methods. The instrumentation and techniques employed to measure the relevant properties of these components will also be discussed. Furthermore, the sample preparation process will be described in detail. Finally, specific experimental details, such as temperature, pressure, and test settings, will be presented to provide a complete understanding of the experimental conditions and results.

3.1 Amines

Monoethanolamine and aminomethyl propanol also known as MEA and AMP were selected for this work based on the supervisors' recommendation and available resources. Table 3.1 presents brief information regarding these two components.

Table 3.1:Brief data for employed amines [8].

Chemical name	Boiling temperature at 101.3 Kpa (℃)	Melting temperature (℃)	Density Kg/m^3 at 20℃	Viscosity mPa.s at 20 ℃	Structure	CAS number
Monoethanolamine	167	4	1016	23.18	H$_2$N⌒OH	141-43-5
Aminomethyl propanol	165	31	934	N.A.	HO⌒NH$_2$	124-68-5

3.2 Mixture preparation

To generate the samples used in the measurement process, a predetermined amount of amine was added to degassed pure water to produce a 100 g mixed sample. Weight measurements were taken using a weight scale with 0.001 g accuracy. Subsequently, the samples were transferred to sealed glass containers and agitated for 20 minutes at 700 revolutions per minute to ensure complete mixing. Finally, the containers were stored in a refrigerated environment at 15 ℃ for subsequent experimentation. The specific details of the prepared samples for each amine are provided in Table 3.2. In these tables, the molecular weights of MEA and pure water are considered to be 61.08 g/mol and 18.015 g/mol, respectively [9].

Table 3.2: Details of prepared MEA samples

$w_{MEA}(g)$	$mole_{MEA}$	$w_{total}(g)$	$w_{H_2O}(g)$	$mole_{H_2O}$	$\dfrac{w_{MEA}}{w_{H_2O}}$	$\dfrac{x_{MEA}}{x_{H_2O}}$
30.028	0.492	100.028	70.000	3.886	0.300	0.112
40.001	0.655	100.010	60.009	3.331	0.400	0.164
50.002	0.819	100.030	50.028	2.777	0.500	0.228

$w_{AMP}(g)$	$mole_{AMP}$	$w_{total}(g)$	$w_{H_2O}(g)$	$mole_{H_2O}$	$\dfrac{w_{AMP}}{w_{H_2O}}$	$\dfrac{x_{AMP}}{x_{H_2O}}$
60.008	0.982	100.004	39.996	2.220	0.600	0.307
70.005	1.146	100.083	30.078	1.670	0.699	0.407
80.002	1.310	100.014	20.012	1.111	0.800	0.541
90.001	1.473	100.020	10.019	0.556	0.900	0.726
30.002	0.337	100.001	69.999	3.886	0.300	0.080
40.007	0.449	100.039	60.032	3.332	0.400	0.119
50.031	0.561	100.003	49.972	2.774	0.500	0.168
60.018	0.673	100.046	40.028	2.222	0.600	0.233
70.009	0.785	100.002	29.993	1.665	0.700	0.321
80.002	0.898	100.009	20.007	1.111	0.800	0.447
90.004	1.010	100.020	10.016	0.556	0.900	0.645
95.00	1.061	100.002	5.403	0.300	0.946	0.779

3.3 Instruments

This section aims to review the instruments used in the experiment, including their capabilities and procedures. The devices and their features will be briefly introduced, followed by a description of their specific tasks relevant to the experiment. It also will be discussed the steps taken during the experiment to ensure accurate and precise measurements.

3.3.1 Density measurement

Density experiments were conducted using an Anton Paar DMA 4500 density meter. The maximum allowable deviation in density was set at 0.0002 g/cm^3. The DMA 4500 was calibrated using the standard calibration procedure with degassed water and air at 20℃. Additionally, the density of pure water was measured three times at different temperatures before and after testing the MEA and AMP samples to ensure the accuracy of the device. Careful attention was given to prevent the presence of air bubbles in the U-tube when inserting the samples. A new sample was used for each composition, and the sample was changed with a new one at each temperature step higher than 50 ℃. Prior to introducing a new sample, the machine was cleaned with ethanol, followed by pure water and dry air.

The MEA samples (as shown in Table 3.2) were tested at 10℃ intervals between 30℃ and 80℃. Meanwhile, AMP samples with a weight fraction of less than 0.9 were tested between 30℃ and 80℃, but for higher concentrations, the lowest temperature was set at 40℃ to prevent crystal formation inside the instrument.

Each experiment was conducted three times to ensure the accuracy of the results.

3.3.2 Viscosity measurement

The dynamic viscosity of the samples was determined using the Anton Paar MCR 101 rheometer, which has a temperature control unit, and the measurements were taken without pressurizing the solution. Regular air checks and motor adjustments were conducted to maintain accuracy. However, during one of the tests, it was discovered that the air check was no longer reliable, leading to the replacement of the machine's bearings. Once the bearing replacement was completed, a new air check was conducted and the results were within acceptable limits, as shown in Figure 3.3. Figure 3.1 shows the initial air check results, while Figure 3.2 shows the results when the machine was not functioning properly. The temperature intervals used for testing the MEA and AMP samples are outlined in Section 3.3.1.

Meas. Pts.	Time [s]	Speed [1/min]	Torque [μNm]	Deflection Angle [°]	Temperature [°C]	Normal Force [N]	Status []
798	400	0.301	0.8395	718	25	******	WMa,Dy_
799	401	0.295	9.643	719	25	******	WMa,Dy_
800	401	0.296	10.89	719	25	******	Dy_accu
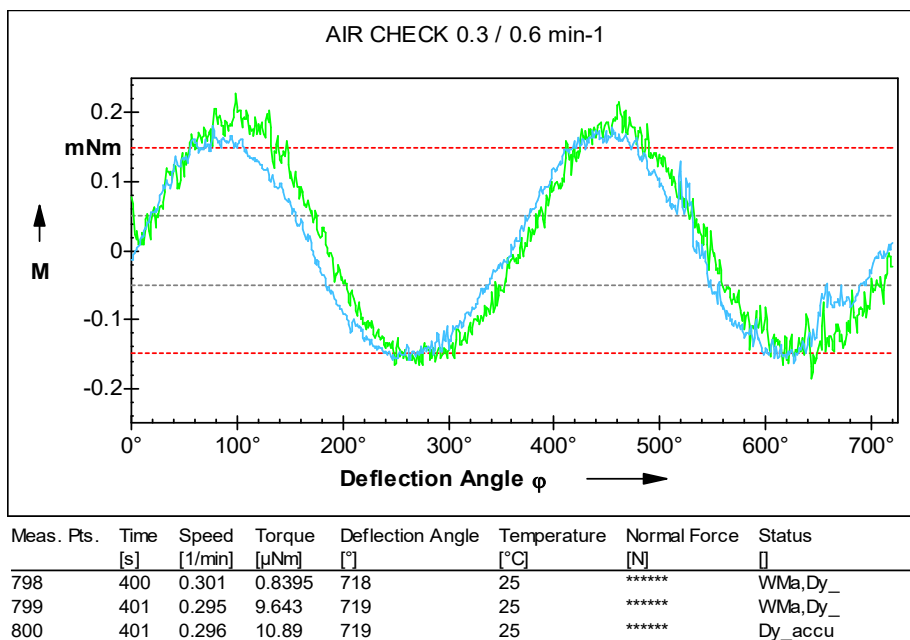
Figure 3.1: Air Check result before stating the measurements

AIR CHECK 0.3 / 0.6 min-1

Meas. Pts.	Time [s]	Speed [1/min]	Torque [µNm]	Deflection Angle [°]	Temperature [°C]	Normal Force [N]	Status []
798	400	0.32	-22.56	718	24.5	******	WMa,Dy_
799	401	0.293	-8.59	718	24.5	******	WMa,Dy_
800	401	0.29	16.93	719	24.5	******	WMa,Dy_
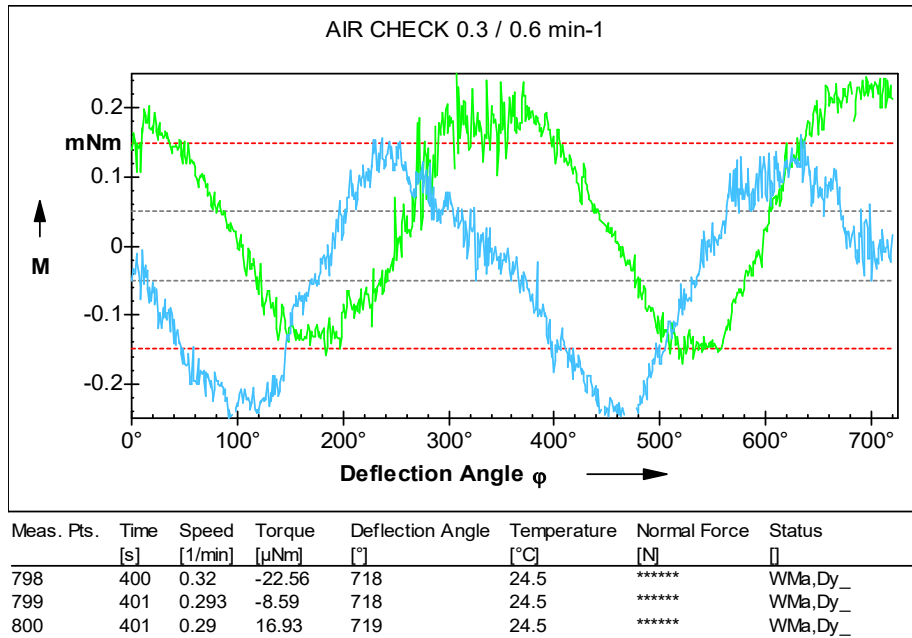
Figure 3.2: Air Check result showing signs of malfunctioning bearings

AIR CHECK 0.3 / 0.6 min-1

Meas. Pts.	Time [s]	Speed [1/min]	Torque [µNm]	Deflection Angle [°]	Temperature [°C]	Normal Force [N]	Status []
721	362	0.301	-36.97	648	27.4	******	WMa,Dy_
722	362	0.299	-35.87	649	27.4	******	WMa,Dy_
723	363	0.3	-36.66	650	27.4	******	WMa,Dy_
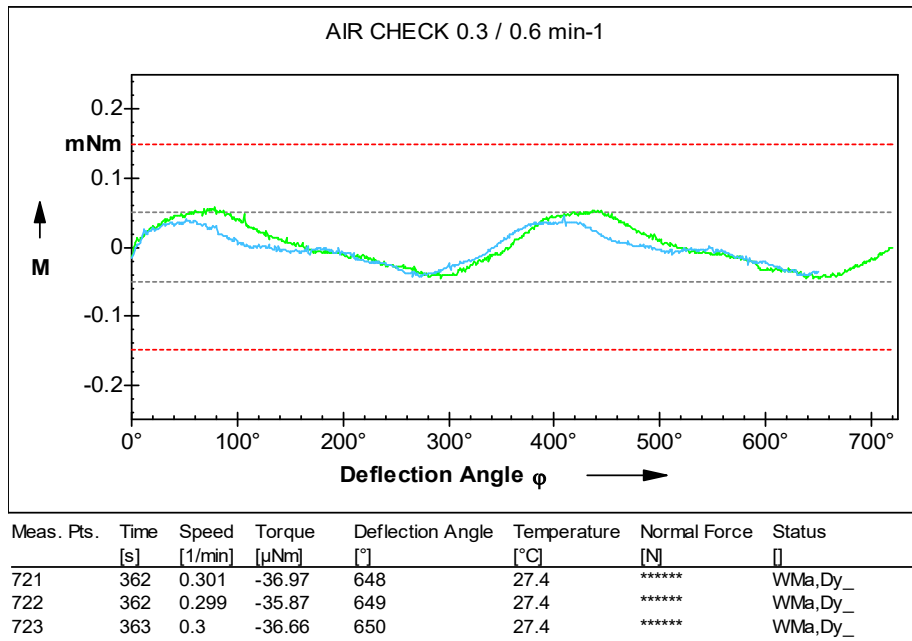
Figure 3.3:Air Check result after changing bearing

After each experiment with a particular sample, the device was allowed to cool down, and the test cell was gently cleaned using pure ethanol, followed by demineralized water. The cell was then left to dry before a new sample was introduced.

4 Laboratory results

This section presents the acquired values for the density of aqueous solutions at various measuring points. Once the data was collected, it was compared with the corresponding values reported in relevant literature sources. The comparison was carried out to identify any discrepancies and evaluate the accuracy of the obtained data. Any differences found were analyzed and explained using possible sources of error or experimental variations.

4.1 Density measurement

4.1.1 Recorded MEA solutions density data

As mentioned earlier, the density of aqueous MEA solutions was measured at weight fractions of MEA ranging from 30% to 100% with 10% intervals. Each sample was tested against a temperature range of 30°C to 80°C with 10°C intervals. Furthermore, each set of experiments was repeated three times to ensure accuracy and consistency of the results.

To avoid any changes in the solution's composition at high temperatures above 50°C, a new sample was injected into the measuring machine after this temperature point. The recorded values are tabulated in table 4.1 and shown as the function of mole fraction change in figure 4.1.

Table 4.1: Recorded values for density of MEA (1) plus water.

T (°C)	MEA weight fraction (w_1)							
	0.3002	0.4000	0.4999	0.6001	0.6995	0.7999	0.8998	1.0000
	MEA mole fraction (x_1)							
	0.1123	0.1643	0.2277	0.3068	0.4070	0.5411	0.7260	1.0000
	$\rho\ (kg/m^3)$							
30	1008.26	1013.42	1018.11	1021.38	1022.69	1020.99	1016.11	1007.93
	1008.24	1013.42	1018.12	1021.37	1022.7	1021	1016.11	1009
	1008.27	1013.42	1018.1	1021.37	1022.71	1020.98	1016.12	1009.2
Mean @ 30	**1008.26**	**1013.42**	**1018.11**	**1021.37**	**1022.70**	**1020.99**	**1016.11**	**1008.71**
40	1003.8	1007.83	1011.82	1014.64	1015.47	1013.5	1008.3	1000
	1003.6	1007.83	1011.82	1014.64	1015.49	1013.5	1008.5	1000.1
	1003.9	1007.82	1011.8	1014.64	1015.46	1013.4	1008.5	1000
Mean @ 40	**1003.77**	**1007.83**	**1011.81**	**1014.64**	**1015.47**	**1013.47**	**1008.43**	**1000.03**
50	998.04	1001.91	1005.73	1007.71	1008.13	1005.88	1000.46	992.03
	998.04	1001.9	1005.7	1007.73	1008.12	1005.86	1000.4	992.02
	998.04	1001.92	1005.75	1007.74	1008.11	1005.86	1000.4	992.03
Mean @ 50	**998.04**	**1001.91**	**1005.73**	**1007.73**	**1008.12**	**1005.87**	**1000.42**	**992.03**
60	992.23	995.65	998.63	999.81	1000.61	998.13	992.45	983.96
	992.24	995.65	998.61	999.84	1000.6	998	992.42	983.94
	992.21	995.65	998.62	999.82	1000.59	998	992.41	983.97
Mean @ 60	**992.23**	**995.65**	**998.62**	**999.82**	**1000.60**	**998.04**	**992.43**	**983.96**
70	985.99	989.01	991.6	992.53	992.8	990.19	984.44	975.92

	986.01	989	991.62	992.52	992.6	990.19	984.46	975.9
	985.08	989	991.63	992.52	992.4	990.17	984.46	975.9
Mean @ 70	**985.69**	**989.00**	**991.62**	**992.52**	**992.60**	**990.18**	**984.45**	**975.91**
	976.55	982.03	984.26	985.49	985.5	982.12	976.29	967.67
80	976.55	982.01	984.25	985.48	985.6	982.12	976.31	967.67
	976.57	982.02	984.23	985.46	985.5	982.12	976.3	967.67
Mean @ 80	**976.56**	**982.02**	**984.25**	**985.48**	**985.53**	**982.12**	**976.30**	**967.67**
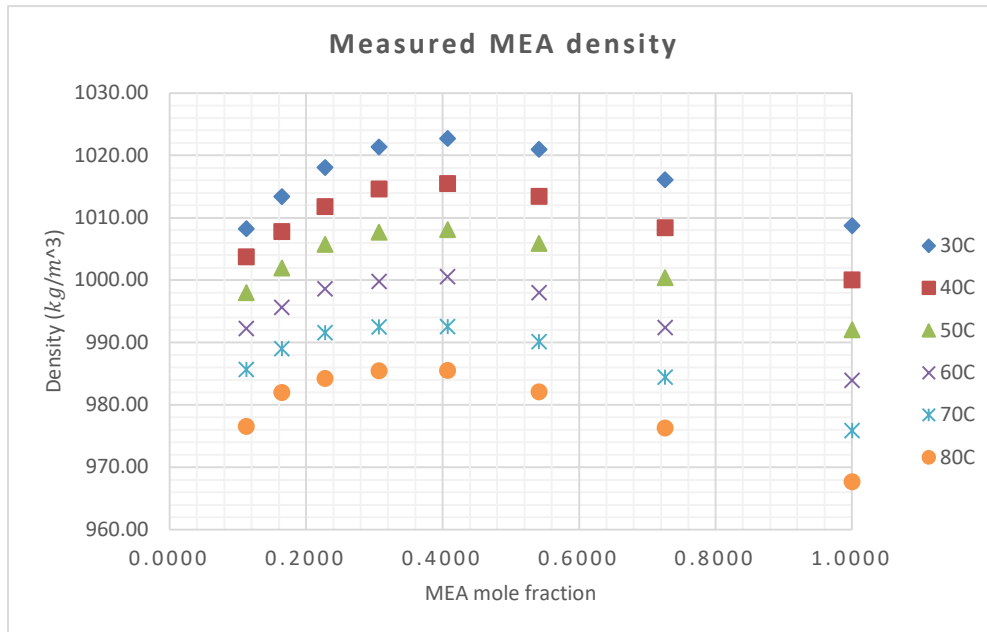
Figure 4.1: plotted density values again MEA mole fraction change

4.1.2 Comparison of MEA density data with literature data

The comparison of our measurements with data from the literature was carried out using one statistical parameter, namely the average absolute relative deviation (AARD). The AARD measures the average difference between our measurements and the literature values as a percentage of the literature values, providing a measure of the overall accuracy of our measurements. The formula for AARD is shown in equation 4.1.

By calculating both AARD, I was able to evaluate the accuracy and precision of my measurements compared to the literature data. The resulting values for absolute relative deviation were then summarized in table 4.2 for further analysis. This table contains the absolute relative deviation for each data point showing the difference with the source in every single condition, however, the AARD and absolute maximum deviation (AMD) is presented based on this data.

$$AARD(\%) = \frac{100\%}{N} \sum_{i=1}^{N} \left| \frac{Y_i^E - Y_i^C}{Y_i^E} \right| \qquad (4.1)$$

19

In equations 4.1, N, Y_i^E, and Y_i^C refer the number of data points, the measured property and literature data for the property respectively.

Table 4.2: Summarized calculation of absolute relative deviation between measured density of MEA (1) +water with litterateur data at each measuring point.

T (°C)		w_1							
		0.3	0.4	0.5	0.6	0.7	0.8	0.9	1
		Absolute relative deviation							
30	Source 1	N.A.	N.A.	N.A.	N.A.	N.A.	N.A.	N.A.	N.A.
	Source 2	0.01%	0.01%	0.03%	0.02%	0.03%	0.02%	0.03%	0.06%
40	Source 1	0.04%	0.01%	0.01%	N.A.	0.00%	N.A.	0.00%	0.03%
	Source 2	0.05%	0.00%	0.02%	0.01%	0.03%	0.02%	0.03%	0.01%
50	Source 1	0.01%	0.01%	0.04%	N.A.	0.01%	N.A.	0.02%	0.03%
	Source 2	0.01%	0.01%	0.05%	0.01%	0.02%	0.02%	0.01%	0.01%
60	Source 1	N.A.	N.A.	N.A.	N.A.	N.A.	N.A.	N.A.	N.A.
	Source 2	0.06%	0.02%	0.02%	0.06%	0.02%	0.01%	0.00%	0.00%
70	Source 1	0.01%	0.01%	0.01%	N.A.	0.04%	N.A.	0.01%	0.01%
	Source 2	0.03%	0.01%	0.02%	0.05%	0.01%	0.02%	0.02%	0.00%
80	Source 1	0.29%	0.01%	0.00%	N.A.	0.05%	N.A.	0.01%	0.01%
	Source 2	0.29%	0.01%	0.01%	0.01%	0.07%	0.02%	0.02%	0.01%

a) Trine et al.
b) Karunarathne et al.

In Table 4.2, the maximum absolute relative deviation at each data point was observed at 0.3 weight fraction and 80 °C, with a value of 0.29%. Furthermore, the AARD was found to be 0.03%. To provide a clearer view, densities were measured and plotted against mole fraction at different temperatures, along with data from both resources, as shown in Figure 4.2. This graph allows for a better visualization of the differences between the measured and literature values across various temperature ranges.

At next step, AARD and absolute maximum deviation (AMD) were calculated between all the data of this work and data from both resources which are 0.029% AARD and 0.284 kg/m^3 AMD in comparing with source 1 and 0.032% AARD and 0.2843 kg/m^3 with source 2.
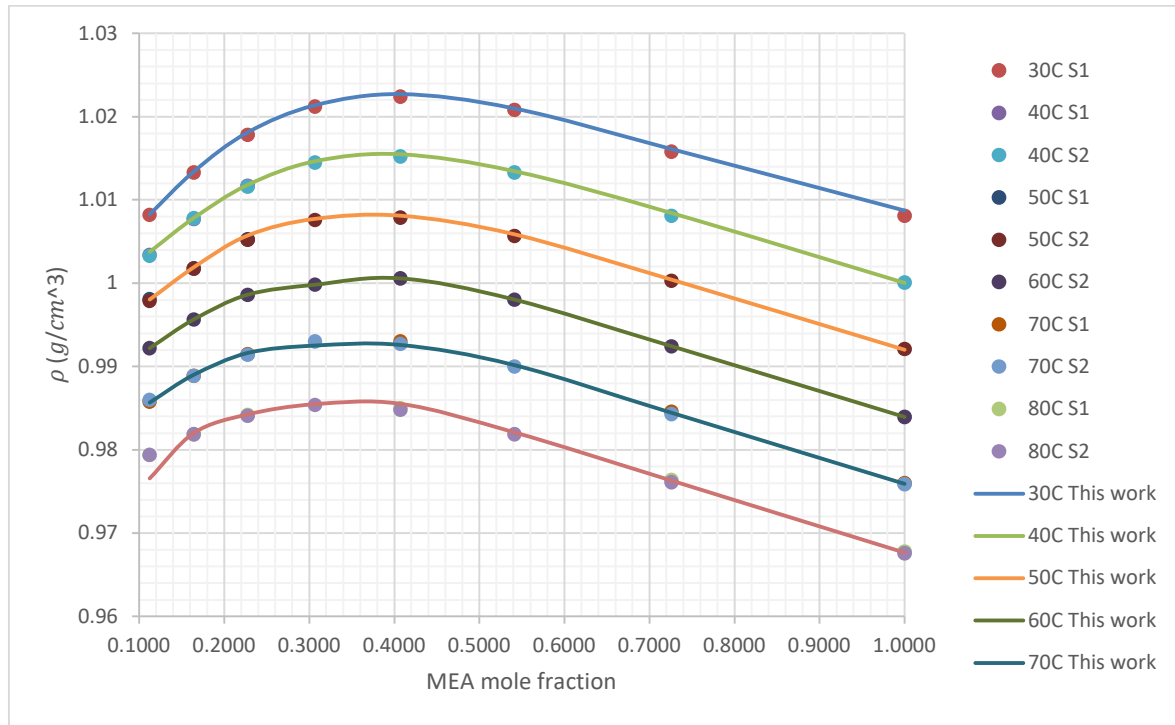
Figure 4.2 plotted measured densities at different temperatures against mole fraction of MEA in comparison of data provided by Trine et al. [6] (S1) and Karunarathne et al. [5] (S2).

4.1.3 Recorded AMP solutions density data

Aqueous AMP solutions were tested for density at different weight fractions of AMP and temperatures. Samples were tested between 30℃ to 80℃, except for concentrations above 90% which started at 40℃ to prevent crystal formation. Each experiment was repeated thrice for accuracy, and a new sample was used above 50℃. Results are in table 4.3 and shown in figure 4.3 as a function of mole fraction change.

Table 4.3: Recorded values for density of AMP (1) plus water.

T (℃)	AMP weight fraction (w_1)								
	30.002	40.007	50.031	60.018	70.009	80.002	90.004	94.599	1.000
	AMP mole fraction (x1)								
	0.080	0.119	0.168	0.233	0.321	0.447	0.645	0.7797	1.000
	$\rho\ (kg/m^3)$								
30	0.9947	0.9930	0.9889	0.9821	0.9726	0.9605	N.A.	N.A.	N.A.
	0.9946	0.9930	0.9889	0.9821	0.9726	0.9605	N.A.	N.A.	N.A.
	0.9947	0.9930	0.9889	0.9822	0.9726	0.9605	N.A.	N.A.	N.A.
Mean @ 30	0.9946	0.9930	0.9889	0.9821	0.9726	0.9605	N.A.	N.A.	N.A.
40	0.9884	0.9860	0.9812	0.9740	0.9645	0.9524	0.9296	0.9377	0.9196
	0.9884	0.9860	0.9812	0.9740	0.9645	0.9524	0.9295	0.9377	0.9196
	0.9884	0.9860	0.9812	0.9740	0.9644	0.9524	0.9296	0.9377	0.9196
Mean @ 40	0.9884	0.9860	0.9812	0.9740	0.9644	0.9524	0.9296	0.9377	0.9196

	0.9822	0.9787	0.9733	0.9659	0.9562	0.9441	0.9212	0.9294	0.9103
50	0.9821	0.9787	0.9733	0.9658	0.9562	0.9441	0.9212	0.9294	0.9103
	0.9822	0.9787	0.9733	0.9658	0.9562	0.9441	0.9212	0.9294	0.9103
Mean @ 50	0.9822	0.9787	0.9733	0.9658	0.9562	0.9441	0.9212	0.9294	0.9103
	0.9750	0.9711	0.9653	0.9575	0.9478	0.9356	0.9127	0.9210	0.9016
60	0.9750	0.9711	0.9653	0.9575	0.9478	0.9356	0.9127	0.9210	0.9016
	0.9750	0.9711	0.9653	0.9575	0.9478	0.9356	0.9127	0.9210	0.9016
Mean @ 60	0.9750	0.9711	0.9653	0.9575	0.9478	0.9356	0.9127	0.9210	0.9016
	0.9631	0.9633	0.9570	0.9490	0.9392	0.9269	0.9039	0.9123	0.8929
70	0.9631	0.9633	0.9569	0.9490	0.9392	0.9269	0.9039	0.9123	0.8929
	0.9631	0.9633	0.9569	0.9490	0.9392	0.9269	0.9039	0.9123	0.8929
Mean @ 70	0.9631	0.9633	0.9569	0.9490	0.9392	0.9269	0.9039	0.9123	0.8929
	0.9478	0.9543	0.9481	0.9402	0.9304	0.9181	0.8950	0.9034	0.8841
80	0.9478	0.9543	0.9480	0.9402	0.9303	0.9180	0.8950	0.9042	0.8841
	0.9478	0.9543	0.9480	0.9402	0.9303	0.9181	0.8950	0.9034	0.8841
Mean @ 80	0.9478	0.9543	0.9480	0.9402	0.9303	0.9180	0.8950	0.9037	0.8841
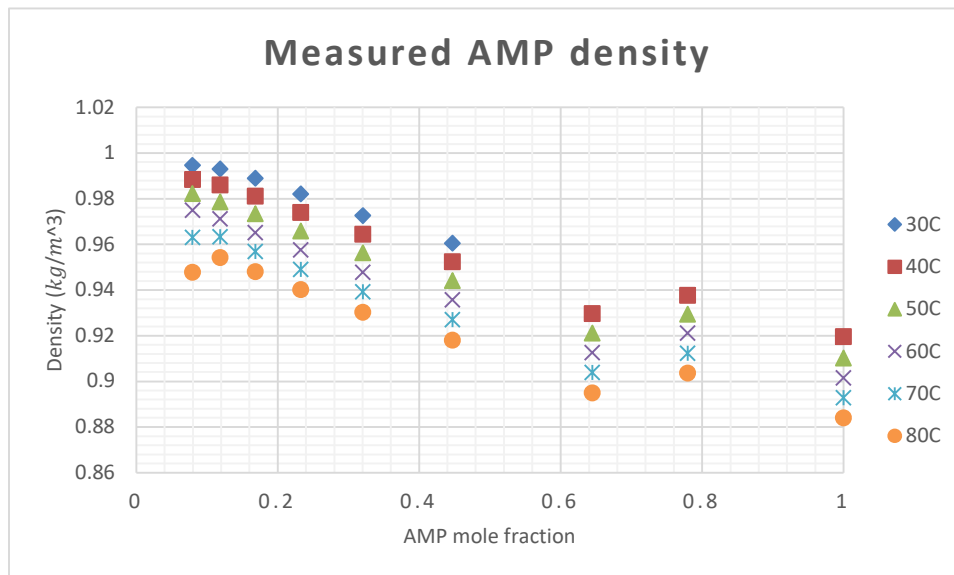
Figure 4.3: plotted density values again AMP mole fraction change

4.1.4 Comparison of AMP density data with literature data

As previously stated, the literature on AMP resources is scarce, making it difficult to verify the results. Specifically, for aqueous AMP solutions, only Henni et al have reported density data for different mole fractions, which is similar to the ones obtained in this experiment. However, due to differences in experimental conditions, a direct comparison between the two data sets is not feasible. Nevertheless, the author used a mathematical model to compare the findings, and the results of this comparison can be found in Table 4.4.

Equation 4.2 [7] presents the correlation proposed by Henni et al, which comprises six coefficients for each temperature increment to estimate the density. The values of these constants are provided in Appendix A for reference.

$$\rho\left(\frac{g}{cm^3}\right) = \sum_{0}^{n} a_k x_1^{\ k} \tag{4.2}$$

Table 4.4: Comparison between measured AMP density compared with densities derived from Henni et al. suggested correlation at each point.

T (°C)		x_1								
		0.07971	0.1187	0.1682	0.2325	0.3205	0.4469	0.6449	0.7796	1
30	ρ_a	0.9946	0.9930	0.9889	0.9821	0.9726	0.9605	N.A.	N.A.	N.A.
	ρ_b	0.9941	0.9918	0.9880	0.9819	0.9727	0.9599	N.A.	N.A.	N.A.
	AARD	0.058%	0.122%	0.096%	0.022%	0.008%	0.066%	N.A.	N.A.	N.A.
40	ρ_a	0.9884	0.9860	0.9812	0.9740	0.9644	0.9524	0.9296	0.9377	0.9196
	ρ_b	0.9884	0.9853	0.9806	0.9737	0.9641	0.9517	0.9367	0.9288	0.9198
	AARD	0.003%	0.069%	0.064%	0.028%	0.032%	0.076%	0.760%	0.958%	0.018%
50	ρ_a	0.9822	0.9787	0.9733	0.9658	0.9562	0.9441	0.9212	0.9294	0.9103
	ρ_b	0.9821	0.9782	0.9728	0.9655	0.9558	0.9433	0.9284	0.9204	0.9113
	AARD	0.010%	0.049%	0.049%	0.030%	0.050%	0.080%	0.772%	0.978%	0.116%
60	ρ_a	0.9750	0.9711	0.9653	0.9575	0.9478	0.9356	0.9127	0.9210	0.9016
	ρ_b	0.9753	0.9708	0.9649	0.9572	0.9472	0.9348	0.9198	0.9118	0.9030
	AARD	0.031%	0.029%	0.033%	0.028%	0.061%	0.089%	0.780%	1.008%	0.152%
70	ρ_a	0.9631	0.9633	0.9569	0.9490	0.9392	0.9269	0.9039	0.9123	0.8929
	ρ_b	0.9678	0.9628	0.9566	0.9489	0.9390	0.9263	0.9107	0.9030	0.8942
	AARD	0.484%	0.048%	0.032%	0.009%	0.028%	0.070%	0.751%	1.030%	0.143%

ρ_a: Density of aqueous AMP experimented in this work (g/cm^3)

ρ_b: Density of aqueous AMP calculated by Henni et al. correlation (g/cm^3)

Referring to table 4.4, maximum average absolute relative deviation is 1.03% and average AARD and AMD are 0.222% and 0.0092 g/cm^3 which shows a consistency between measured value and the model at each point.

4.2 Viscosity measurement

4.2.1 Recorded Viscosity data of aqueous MEA

As mentioned in section 3.3.2, measurements were taken to determine the viscosity of aqueous MEA solutions. Weight fractions of MEA were varied from 30% to 100%, with 10% intervals, and each sample was subjected to a temperature range of 30℃ to 80℃, with 10℃ intervals. The rheometer device was configured to take 20 measurements at each temperature step, with a 20-second interval between measurements, to ensure that the results were more accurate. The viscosity of each sample at each temperature step was calculated by taking a normal average of the 20 measured points.

The summarized measured value for MEA solution is tabulated in table 4.5 and visualized in figure 4.4. Furthermore, details of measurement driven from the rheometer device can be found in appendix B.

Table 4.5: Measured viscosity of MEA + water at different mole fraction of MEA(x_1) and temperatures.

T (℃)	x_1							
	0.112314	0.164304	0.227675	0.30677	0.407046	0.541096	0.72599	1
	$\eta \ (mPa.s)$							
30	2.112333	3.2547	4.771233	6.6926	9.7273	12.7985	14.898	14.698
40	1.658567	2.4674	3.522133	4.72725	6.59515	8.54765	9.9105	9.9987
50	1.316333	2.012633	2.718233	3.44265	4.64905	5.9739	6.84495	6.927
60	1.081733	1.80222	1.99	2.56325	3.3967	4.2661	4.9031	5.049
70	0.906477	1.5553	1.571	1.9861	2.5793	3.1675	3.6252	3.817
80	0.76128	1.2545	1.2334	1.5595	1.99485	2.42215	2.74935	2.963
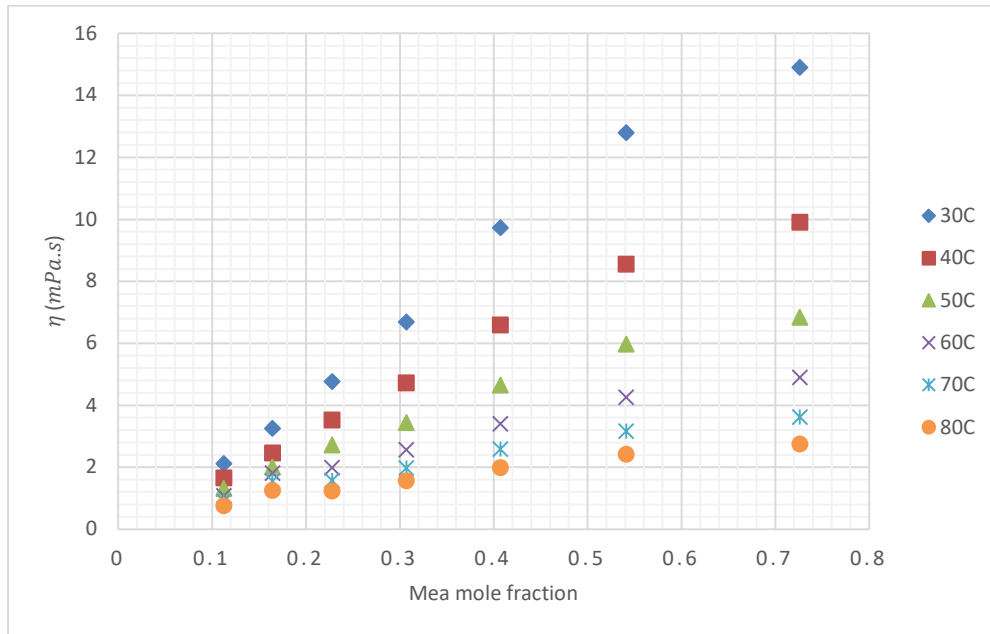
Figure 4.4: plotted viscosity values again MEA mole fraction (x_1) change.

4.2.2 Comparison of MEA viscosity data with literature data

In this section, the Average Absolute Relative Deviation (AARD) as defined in section 4.1.1.1, to measure the average difference between our measurements and the literature values as a percentage of the literature values. The resulting AARD values were then summarized in Table 4.6 for further analysis.

Table 4.6: Summarized calculation of AARD between measured viscosity of MEA (1)+water with litterateur data.

T (°C)		w_1							
		0.3	0.4	0.5	0.6	0.7	0.8	0.9	1
		AARD							
30	Source 2	0.16%	3.22%	4.01%	1.14%	0.98%	0.32%	0.44%	0.34%
40	Source 1[a]	0.69%	7.60%	3.75%	N.A.	5.53%	N.A.	2.92%	3.89%
	Source 2[b]	1.84%	2.88%	6.02%	0.19%	1.04%	0.16%	0.32%	1.09%
50	Source 1	1.04%	13.05%	6.56%	N.A.	6.26%	N.A.	3.14%	2.99%
	Source 2	2.00%	0.53%	9.72%	0.04%	1.53%	0.62%	0.23%	0.12%
60	Source 2	3.30%	4.18%	3.77%	1.51%	1.89%	0.68%	0.67%	0.36%
70	Source 1	1.49%	26.70%	0.06%	N.A.	8.17%	N.A.	5.10%	3.33%

	Source 2	4.47%	3.62%	2.74%	2.26%	1.38%	1.56%	1.59%	0.45%
80	Source 1	1.15%	24.27%	3.78%	N.A.	9.28%	N.A.	6.57%	3.81%
	Source 2	2.80%	4.16%	0.78%	3.88%	1.71%	2.51%	3.01%	0.37%

a) Trine et al.

b) Karunarathne et al.

In this comparison, a maximum AARD of 26.70% was obtained with source one when comparing each data point, while the average AARD was 6.07%. These results suggest a significant difference that may be due to the use of different measuring devices, which will be further investigated in the conclusion section. Regarding source two, the maximum AARD was found to be 9.27% in point-by-point comparison, with an average AARD of 1.93%, which is more consistent with the results of our study. The AMD evaluated to be 0.642 and 0.415 mPa.s. To provide a better overview, the results of both sources and this work have been plotted in Figures 4.5 and 4.6.
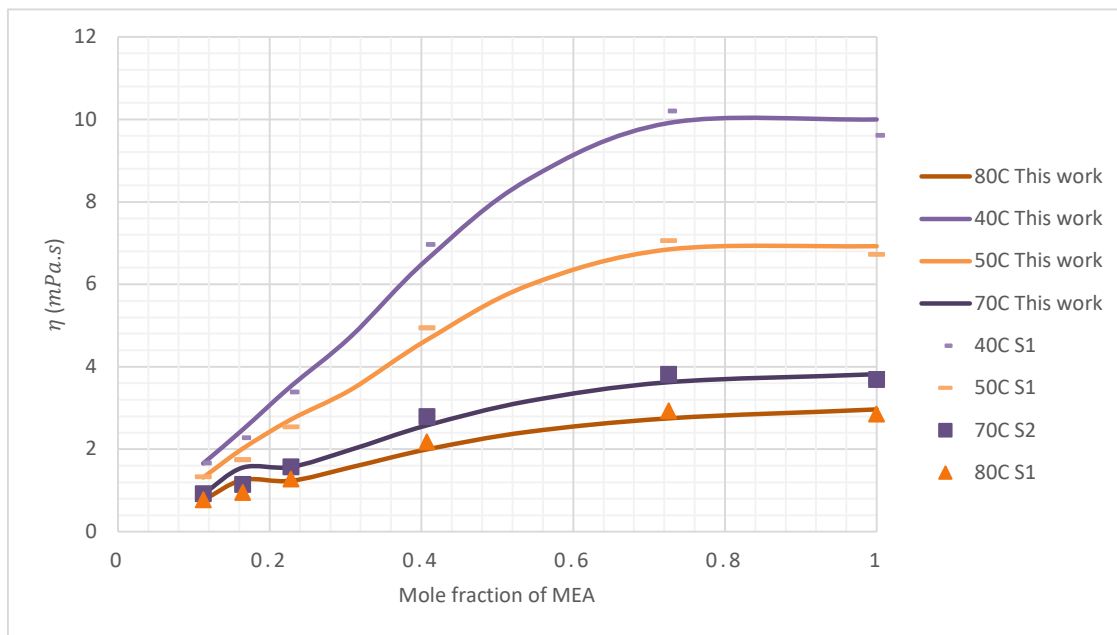
Figure 4.5: Comparison between measurements of viscosity of aqueous MEA this work and Trine et al. (S1).
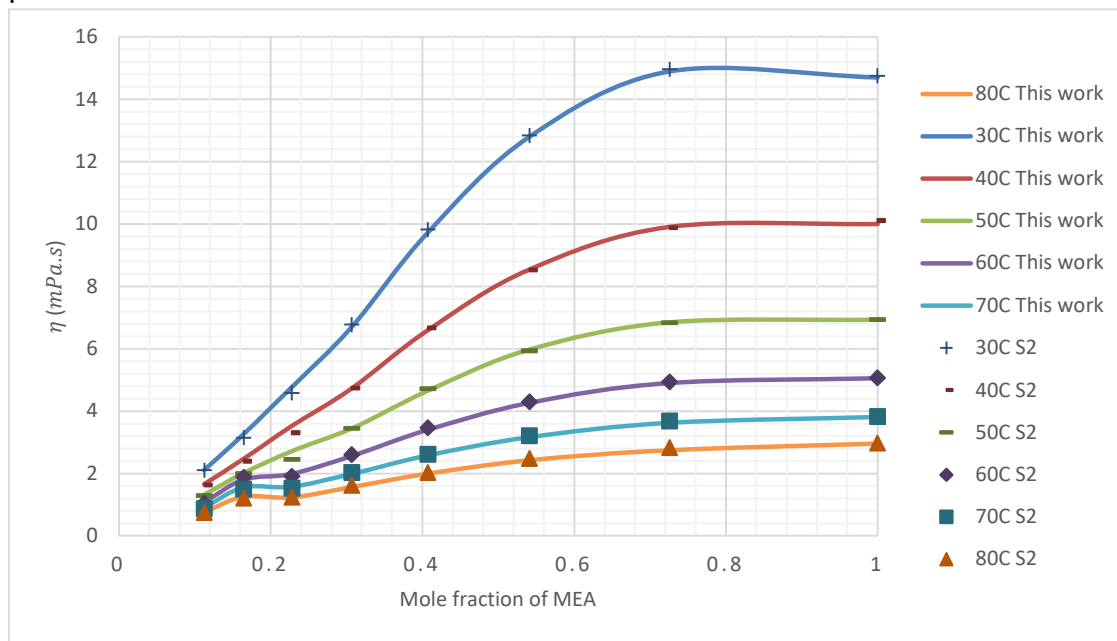
Figure 4.6: comparison between measurements of viscosity of aqueous MEA this work and Karunarathne et al. (S2).

4.2.3 Recorded Viscosity data of aqueous AMP

The viscosity of AMP was measured using similar procedures to those described in Section 4.2.1, with the exception that a start temperature of 40 °C was used for weight fractions higher than 60% and to prevent crystal formation and protect the device. The measured values for the AMP solution are summarized in Table 4.7 and displayed graphically in Figure 4.7. Additional information regarding the measured data can be found in Appendix B.

Table 4.7: Measured viscosity of AMP + water at different mole fraction of AMP (x_1) and temperatures.

T (°C)	x_1								
	0.0797	0.1187	0.1682	0.2325	0.3205	0.4469	0.6449	0.7797	1.00
	$\eta \ (mPa.s)$								
30	3.0056	4.8733	6.6261	13.873	N.A.	N.A.	N.A.	N.A.	N.A.
40	2.1748	3.3381	5.3678	8.5492	14.029	23.559	31.176	46.448	47.2
50	1.6306	2.4043	3.7011	5.607	8.7953	13.909	17.966	25.067	25.34
60	1.2530	1.7610	2.6611	3.8810	5.8150	8.6998	10.970	14.4795	14.51
70	0.9901	1.3366	2.0066	2.8010	4.0433	5.7503	7.0823	8.9555	9.001

| 80	0.7979	1.0396	1.5605	2.0897	2.9450	3.9716	4.7930	5.8568	5.984
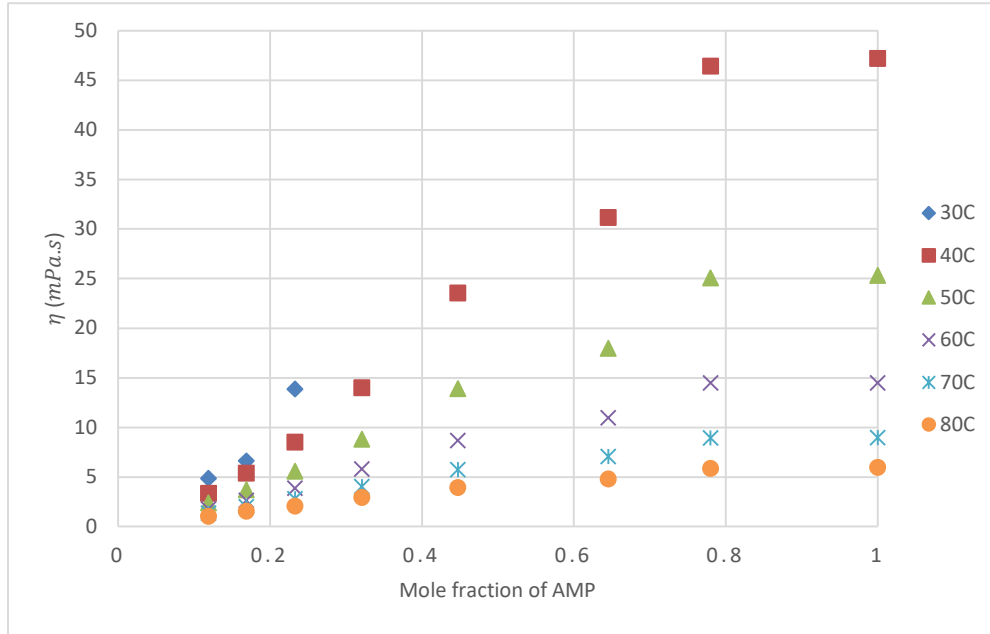
Figure 4.7: Plotted viscosity values again AMP mole fraction (x_1) change.

4.2.4 Comparison of AMP viscosity with literature data

Because of the same issue regarding the lack of data at our measured points, the same procedure as for AMP density was followed, which involved calculating viscosity based on a suggested correlation and comparing the measured viscosity with those calculated values. This comparison was made by calculating AARD, as presented in Table 4.8. The viscosity was estimated using equation 4.3 proposed by Henni et al. [7] , which includes six coefficients for each temperature increment. The values of these constants are provided in Appendix A for reference.

$$\ln \eta \, (mpa.s) = \ln \eta_0 + \sum_0^n a_k x_1^{\,k} \qquad (4.3)$$

In equation 4.3, a_k are constants which can be found in appendix B, η_0 referee to pure water viscosity which considered 0.797, 0.653, 0.552, 0.476 , and 0.418 mPa.s respectively for temperature range of 40°C up to 70°C [10].

Table 4.8:Comparison between measured AMP viscosity compared with data derived from Henni et al. suggested correlation.

T (°C)	x_1							
	0.1187	0.1682	0.2325	0.3205	0.4469	0.6449	0.7797	1.00
	AARD							
40	4.075%	2.761%	3.044%	1.674%	0.493%	27.310%	0.083%	4.962%
50	4.313%	2.836%	3.387%	1.315%	0.166%	21.482%	0.594%	3.812%
60	6.267%	2.826%	3.450%	1.940%	1.419%	18.562%	0.430%	2.924%
70	11.835%	4.487%	4.457%	0.909%	0.046%	16.052%	2.247%	5.801%

In table 4.8, highest number for AARD recorded is 27.310% and the average value for whole data set is 5.186% and the AMD found to be 8.51 mPa.s.

5 Data fitting and Correlations

In this part of the report, an attempt is made to suggest some mathematical correlations which can describe the data acquired from experiments by a model. This would enable the prediction of the property of solvents at different mole fractions or temperatures other than the experimented conditions, which can be helpful in more sophisticated calculations used in carbon capture processes as mentioned in section 1 of this report.

The offered models are often chosen from well-known correlations which are more likely to comply with the performed test condition of this work. It is attempted to offer more than one correlation for each set of data. While some of the models comply with the experimental data, in some cases, the proposed model does not have satisfactory comparison scales.

In this section, the calculations were performed using Microsoft Excel and its built-in functions. Curve fitting was carried out using the built-in function called curve fitter in MATLAB R2022b.

The detailed tables of calculated parameters along with relevant MATLAB codes for this chapter can be found in appendix C for density data and D for viscosity data. due to the similarity in codes, only one sample for each model is placed in the appendix files.

5.1 Density data fitting and mathematical correlations

To model the density data, two correlations were utilized: the first was based on a Redlich-Kister [11] type polynomial to predict excess volume, while the second was based on a model suggested by Aronu, Hartono, and Svendsen [12], which will be referred to as the Aronu model in this work.

5.1.1 Redlich-Kister model for excess molar volume

Redlich and Kister introduced an algebraic representation for the excess thermodynamic properties of nonelectrolyte solutions, which involves representing the excess molar volume as a power series with temperature-dependent parameters. This approach has been utilized to correlate excess molar volumes for the binary mixture of amin and water. The effect of temperature on the excess volume is accounted for by including a linear function for the parameters in the Redlich-Kister correlation as shown in equation 5.1 [11].

$$v^E_{m=}x_1(1-x_1)\sum_{i=0}^{i=n}A_i(1-2x_1)^i$$

$$A_i = a_{i0} + a_{i1}(T)$$

(5.1)

In equation 5.1, x_1 refers to mole fraction of the amine, T is solvent temperature in Celsius degree, and v^E_m is excess molar volumes which is defined as equation 5.2.

$$v^E_{m=}v_m - (v^0_1 \times x_1 + v^0_2 \times x_2) \tag{5.2}$$

In equation 5.2, v_m refers to molar volume of the aqueous mixture and v^0_i is the molar volume of pure component in the mixture [13].

5.1.1.1 Redlich-Kister model for aqueous MEA solutions density

In light of the aforementioned descriptions and the experimental density data presented in Table 4.1, the calculation of excess molar volume is carried out according to the methodology outlined in Table 5.1. To obtain the final parameter, additional intermediate calculations, aside from Equations 5.1 and 5.2, are performed. Specifically, the molar weight of the mixture and the molar volume of the mixture are computed using Equations 5.3 and 5.4, respectively.

$$M_{mix} = \sum_1^n M_i \tag{5.3}$$

$$v_{mix} = \frac{M_{mix}}{\rho_{mix}} \tag{5.4}$$

Table 5.1: Calculated excess molar volume at each temperature and mole fraction of MEA (x_1).

T (°C)	x_1	$v^E_m (m^3/mole)$	T (°C)	x_1	$v^E_m (m^3/mole)$
30	0.1123	-2E-07	50	0.5411	-5.1E-07
30	0.1643	-3.1E-07	50	0.726	-3.8E-07
30	0.2277	-4.4E-07	50	1	0
30	0.3068	-5.5E-07	60	0.1123	5.22E-08
30	0.407	-6.2E-07	60	0.1643	-6.8E-08
30	0.5411	-6E-07	60	0.2277	-2E-07
30	0.726	-4.2E-07	60	0.3068	-3.1E-07
30	1	0	60	0.407	-4.4E-07
40	0.1123	-8.6E-08	60	0.5411	-4.7E-07
40	0.1643	-1.9E-07	60	0.726	-3.5E-07
40	0.2277	-3.2E-07	60	1	0
40	0.3068	-4.5E-07	70	0.1123	1.31E-07
40	0.407	-5.4E-07	70	0.1643	1.48E-09
40	0.5411	-5.5E-07	70	0.2277	-1.4E-07

40	0.726	-4.1E-07	70	0.3068	-2.5E-07
40	1	0	70	0.407	-3.7E-07
50	0.1123	-1.4E-08	70	0.5411	-4.2E-07
50	0.1643	-1.3E-07	70	0.726	-3.3E-07
50	0.2277	-2.7E-07	70	1	0
50	0.3068	-3.9E-07	80	0.1123	2.66E-07
50	0.407	-4.9E-07	80	0.1643	7.41E-08

By utilizing the calculated excess molar volume, temperature points, and mole fractions, the MATLAB curve fitter application can fit the data into a curve employing a 3rd order Redlich-Kister polynomial. The resulting curve boasts a notable R-squared value of 0.9925, as demonstrated in Figure 5.1. The coefficients of the correlation are further presented in Table 5.2.

To ensure the accuracy of the curve fitting, a reverse calculation is conducted, wherein the excess molar volume is determined at available temperature and mole fraction points. This process, in turn, yields a new density value. Subsequently, tools such as Average Absolute Relative Deviation (AARD) and Absolute Mean Deviation (AMD) are employed to determine the quality of the correlation. The calculated values for this fitting reveal an AARD of 0.047% and an AMD of 2.85 (Kg/m^3), indicating highly accurate data fitting.

Table 5.2: Calculated coefficients of Redlich-Kister polynomial for aqueous MEA from 30 °C up to 80 °C.

Coefficient	Value	Coefficient	Value	Goodness of the fit
a_{00}	-3.03E-06	a_{20}	1.65E-07	
a_{01}	1.93E-08	a_{21}	1.92E-08	R^2=0.9925
a_{10}	-7.52E-07	a_{30}	-1.56E-06	AARD=0.047%
a_{11}	6.31E-09	a_{31}	9.02E-08	AMD= 2.85 (Kg/m^3)
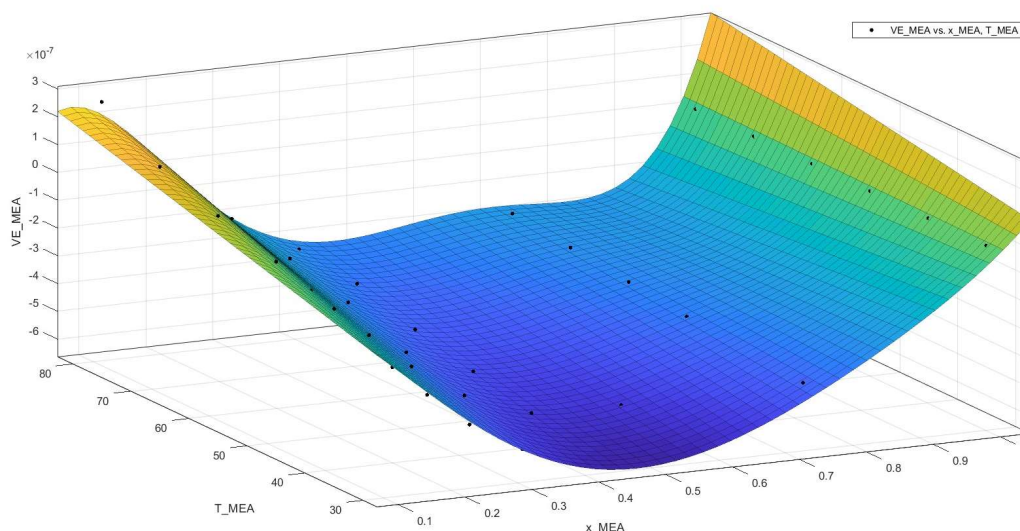
Figure 5.1: Fitted curve for aqueous MEA data using MATLAB (Redlich-Kister polynomial).

5.1.1.2 Redlich-Kister model for aqueous AMP solutions density

To analyze the behavior of an AMP plus water solution, a similar methodology as that used for aqueous MEA is adopted. However, due to the need for a consistent chain of data points to create a fitted curve, Redlich-Kister model for AMP is developed for temperature range of 40℃ up to 80℃.

The result of calculating excess molar volume for AMP solution at specified temperature range and mole fractions are tabulated in table 5.3.

Table 5.3: Calculated excess molar volume at each temperature and mole fraction of AMP (x_1).

T (℃)	x_1	$v_m^E(m^3/mole)$	T (℃)	x_1	$v_m^E(m^3/mole)$
40	0.08	-3.454E-07	60	0.321	-8.846E-07
40	0.119	-5.516E-07	60	0.447	-9.295E-07
40	0.168	-7.353E-07	60	0.645	-1.698E-07
40	0.233	-8.927E-07	60	0.7797	-1.287E-06
40	0.321	-9.940E-07	60	1	0.000E+00
40	0.447	-9.944E-07	70	0.08	2.002E-08
40	0.645	-1.883E-07	70	0.119	-2.950E-07
40	0.7797	-1.195E-06	70	0.168	-4.763E-07
40	1	0.000E+00	70	0.233	-6.598E-07
50	0.08	-2.772E-07	70	0.321	-8.121E-07

50	0.119	-4.729E-07	70	0.447	-8.709E-07
50	0.168	-6.574E-07	70	0.645	-1.163E-07
50	0.233	-8.252E-07	70	0.7797	-1.282E-06
50	0.321	-9.516E-07	70	1	0.000E+00
50	0.447	-9.796E-07	80	0.08	3.157E-07
50	0.645	-2.018E-07	80	0.119	-1.752E-07
50	0.7797	-1.269E-06	80	0.168	-3.693E-07
50	1	0.000E+00	80	0.233	-5.687E-07
60	0.08	-1.859E-07	80	0.321	-7.314E-07
60	0.119	-3.844E-07	80	0.447	-8.074E-07
60	0.168	-5.712E-07	80	0.645	-6.292E-08
60	0.233	-7.444E-07	80	0.7797	-1.295E-06

By following the same procedure as MEA but with higher order of Redlich-Kister polynomial a curve with R-squared value of 0.9624, as demonstrated in Figure 5.2 will fit to the data. The coefficients of the correlation are presented in Table 5.4. the AARD and AMD for these set of data are 0.158% and 10.55 (Kg/m^3).

Table 5.4: Calculated coefficients of Redlich-Kister polynomial for aqueous AMP from 40 ℃ up to 80 ℃.

Coefficient	Value	Coefficient	Value	Goodness of the fit
a_{00}	-3.89E-06	a_{21}	-1.18E-07	
a_{01}	2.54E-08	a_{30}	3.24E-05	R^2=0.9624
a_{10}	-1.02E-05	a_{31}	1.34E-07	AARD=0.158%
a_{11}	7.81E-09	a_{40}	-4.96E-05	AMD= 10.55 (Kg/m^3)
a_{20}	6.69E-06	a_{41}	2.88E-07	
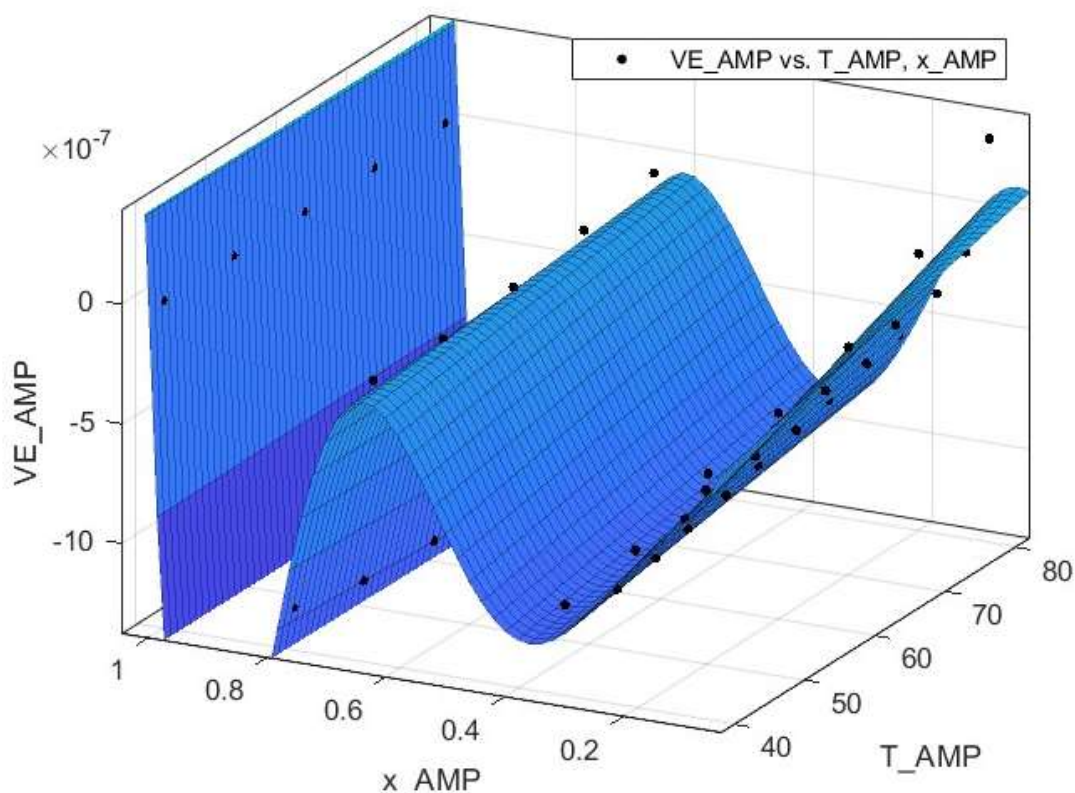
Figure 5.2:Fitted curve for aqueous AMP data using MATLAB (Redlich-Kister polynomial).

5.1.2 Aronu model

Aronu, Hartono, and Svendsen proposed a correlation, as presented in Equation 5.3, that can directly relate temperature and mole fraction to density [12]. In contrast to the Redlich-Kister model, which requires semi-complex calculations and is indirect, the Aronu model provides a more straightforward approach for calculating density. This model involves four coefficients (k_i) that require estimation by curve fitting, as shown in the equation.

$$\rho = \left(k_1 + \frac{k_2(1 - x_1)}{T}\right) \exp\left(\frac{k_3}{T} + \frac{k_4 x_1}{T} + k_5 \left(\frac{x_1}{T}\right)^2\right) \tag{5.3}$$

In this equation, x_1 refers to mole fraction of the amine, unit of density is kilogram per square meter and temperature is stated in Kelvin.

5.1.2.1 Aronu model for aqueous MEA solutions density

Considering the fact that this model directly calculates the density, it is enough to enter values for Measured density, temperature and mole fractions in to the MATLAB curve fitter.

Table 5.6 includes the coefficients of Aronu model fitted to aqueous MEA data for temperature range of 30 °C to 80 °C and the visual result is illustrated in figure 5.3.

Table 5.5: Calculated coefficients of Aronu model for aqueous MEA from 30 ℃ up to 80 ℃.

Coefficient	Value	Goodness of the fit
k_1	771.10	
k_2	1.05E+05	R^2=0.9741
k_3	-30.91	AARD=0.1806%
k_4	109.00	AMD= 5.46 (Kg/m^3)
k_5	858.60	

Figure 5.3: Fitted curve for aqueous MEA data using MATLAB (Aronu model).

5.1.2.2 Aronu model for aqueous AMP solutions density

By following same procedure as in section 5.1.2.1, coefficients for AMP solution model based on Aronu model can be calculated as in table 5.6. The result of the fitter curve is reflected in figure 5.4.

Table 5.6:Calculated coefficients of Aronu model for aqueous AMP from 40 ℃ up to 80 ℃.

Coefficient	Value	Goodness of the fit
k_1	701.30	
k_2	-5.04E+04	R^2=0.9753
k_3	193.70	AARD=0.123%
k_4	-136.20	AMD= 9.24 (Kg/m^3)

k$_5$	8858.60	
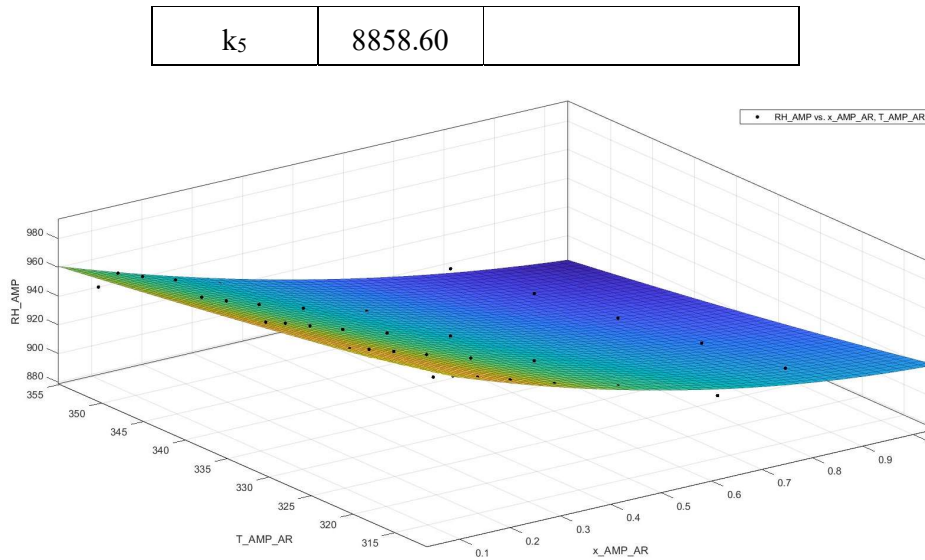
Figure 5.4: Fitted curve for aqueous AMP data using MATLAB (Aronu model).

5.2 Viscosity data fitting and mathematical correlations

In this study, the researchers employed two of the most famous viscosity models, namely the Eyring's viscosity model based on absolute rate theory and the Arrhenius equation, to describe the viscosity data mathematically. These models were chosen for the same reason as in the density section. Specifically, the Arrhenius equation directly calculates viscosity from temperatures and weight fraction, while the other model uses excess property to provide viscosity data.

5.2.1 Eyring's viscosity model for simulating viscosity data

In this study Eyring's viscosity model described in equation (5.4) is used to study the viscosity of non-aqueous mixtures [13].

$$\eta = \frac{hN_A}{V} \exp\left(\frac{\Delta G^*}{RT}\right) \tag{5.4}$$

Where η is the dynamic viscosity, V is molar volume, h is Planks constant, N_A is Avogadro's number, $\Delta G^* is$ free energy of activation for viscous flow, R is universal gas constant and T is temperature.

To study the difference between the measured viscosity and ideal viscosity of the mixtures, the term excess free energy of activation for viscous flow(ΔG^{E*}) is used. Equation (5.4) is utilized to derive the equation (5.5) and equation (5.6) [5].

$$\frac{\eta}{\eta_{ideal}} = \frac{V_{ideal}}{V} \exp\left(\frac{\Delta G^{E*}}{RT}\right) \tag{5.5}$$

$$\frac{\Delta G^{E*}}{RT} = \ln(\eta V) - \sum_{i=1}^{i=2} x_i \ln (\eta_i V_i^0) \qquad (5.6)$$

Where x_i is mole fraction of components, η_i is dynamic viscosity of pure components, V_i^0 is molar volume of pure components.

A Redlich-Kister polynomial in the form of Equation 5.7 and 5.8 can be used to fit the calculated values to a curve.

$$\frac{\Delta G^{E*}}{RT} = x_1(1 - x_1) \sum_{i=1}^{i=2} C_i (1 - 2x_1)^i \qquad (5.7)$$

$$C_i = a_i + b_i(T) \qquad (5.8)$$

5.2.1.1 Eyring's viscosity model for aqueous MEA data

As described in section 5.2.1, the excess free energy of activation for viscous flow is calculated and tabulated in table 5.7, and then, using these values and MATLAB curve fitting, the values for ΔG^{E*} were fitted to a Redlich-Kister polynomial as illustrated in figure 5.5 with characteristics as shown in table 5.8.

As it is notable in the result, however a second order of temperature depended coefficient chosen for this work, the results for this fitting are not satisfactory.

Table 5.7: Calculated excess free energy of activation for MEA(1)+ water solution

T (°C)	x_1	ΔG^{E*}	T (°C)	x_1	ΔG^{E*}	T (°C)	x_1	ΔG^{E*}
303.15	0.112	1859.978	343.15	0.228	2198.430	323.15	0.541	2943.441
313.15	0.112	1661.993	353.15	0.228	362.018	333.15	0.541	2700.663
323.15	0.112	1447.268	303.15	0.307	3499.470	343.15	0.541	2482.601
333.15	0.112	1283.638	313.15	0.307	3222.261	353.15	0.541	1362.647
343.15	0.112	1134.102	323.15	0.307	2966.594	303.15	0.726	2321.441
353.15	0.112	-818.457	333.15	0.307	2699.315	313.15	0.726	2146.277
303.15	0.164	2631.827	343.15	0.307	2475.305	323.15	0.726	2012.979
313.15	0.164	2407.233	353.15	0.307	844.049	333.15	0.726	1861.689
323.15	0.164	2327.032	303.15	0.407	3722.728	343.15	0.726	1706.315
333.15	0.164	2460.917	313.15	0.407	3417.991	353.15	0.726	1002.078
343.15	0.164	2458.800	323.15	0.407	3153.032	303.15	1.000	-1.525
353.15	0.164	549.754	333.15	0.407	2898.441	313.15	1.000	0.182
303.15	0.228	3185.722	343.15	0.407	2678.718	323.15	1.000	0.190

313.15	0.228	2956.417	353.15	0.407	1259.678	333.15	1.000	0.113
323.15	0.228	2790.120	303.15	0.541	3404.356	343.15	1.000	-0.029
333.15	0.228	2420.854	313.15	0.541	3144.830	353.15	1.000	-0.212

Table 5.8: Calculated coefficients of Eyring's viscosity model for aqueous MEA from 303.15 K up to 333.15 K.

Coefficient	Value	Goodness of the fit
a_0	-59.01	
a_1	148	
a_2	-387.1	
b_0	0.4521	R^2=0.9476
b_1	-0.963	AARD=17.69%
b_2	2.415	AMD= 4.347 $(m.Pa.s)$
c_0	-0.0007891	
c_1	0.001542	
c_2	-0.003756	
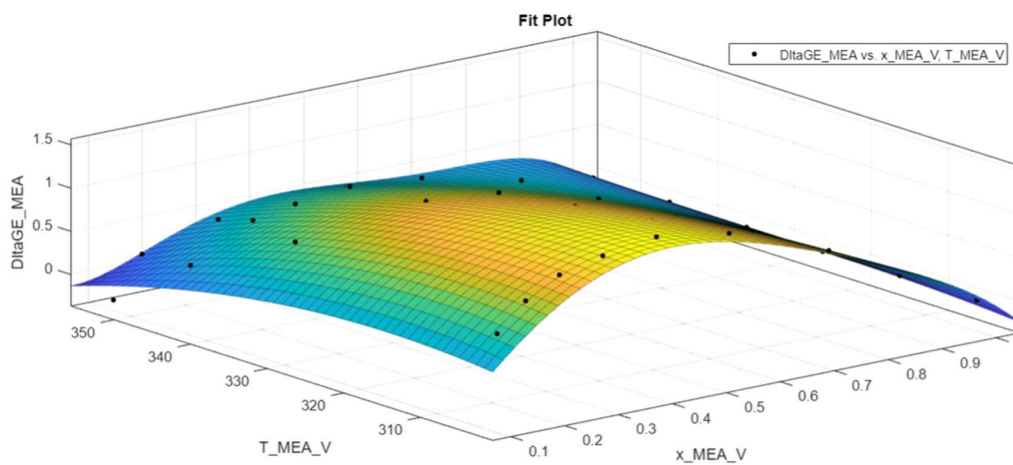
Figure 5.5:Fitted curve for aqueous MEA data using MATLAB (Eyring's viscosity model).

5.2.1.2 Eyring's viscosity model for aqueous AMP data

By conducting the same evaluations as those carried out for aqueous MEA, the excess free energy of activation for AMP flow was calculated in the first step, and the results were tabulated in table 5.9. Subsequently, a Redlich-Kister polynomial was fitted to these findings

using three sets of coefficients and a second-order temperature-dependent coefficient. However, the R-square value did not exceed 0.921, indicating insufficient accuracy for this model. The details of the coefficients and fitness characteristics are presented in table 5.10, while the related curve is illustrated in figure 5.7.

Table 5.9: Calculated excess free energy of activation for AMP (1) + water solution

T (°C)	x_1	ΔG^{E*}	T (°C)	x_1	ΔG^{E*}	T (°C)	x_1	ΔG^{E*}
313.15	0.0797	1.441	343.15	0.1683	1.760	323.15	0.4470	2.337
323.15	0.0797	1.299	353.15	0.1683	1.084	333.15	0.4470	2.171
333.15	0.0797	1.170	313.15	0.2326	2.478	343.15	0.4470	2.023
343.15	0.0797	1.061	323.15	0.2326	2.286	353.15	0.4470	1.514
353.15	0.0797	0.336	333.15	0.2326	2.123	313.15	0.6449	1.714
313.15	0.1187	1.845	343.15	0.2326	1.979	323.15	0.6449	1.615
323.15	0.1187	1.684	353.15	0.2326	1.327	333.15	0.6449	1.515
333.15	0.1187	1.525	313.15	0.3205	2.613	343.15	0.6449	1.419
343.15	0.1187	1.387	323.15	0.3205	2.423	353.15	0.6449	1.093
353.15	0.1187	0.660	333.15	0.3205	2.255	313.15	0.7797	1.321
313.15	0.1683	2.217	343.15	0.3205	2.108	323.15	0.7797	1.229
323.15	0.1683	2.040	353.15	0.3205	1.522	333.15	0.7797	1.135
333.15	0.1683	1.886	313.15	0.4470	2.519	343.15	0.7797	1.050

Table 5.10:Calculated coefficients of Eyring's viscosity model for aqueous AMP from 313.15 K up to 333.15 K.

Coefficient	Value	Coefficient	Value	Goodness of the fit
a_0	51.590	b_2	6.4970	
a_1	29.890	b_3	-6.1460	
a_2	-47220.0	c_0	2.41E-04	R^2=0.921
a_3	994.40	c_1	4.49E-04	AARD=76.6%
b_0	-0.21370	c_2	-1.01E-02	AMD= 43.013 $(m.Pa.s)$
b_1	-0.25630	c_3	9.49E-03	
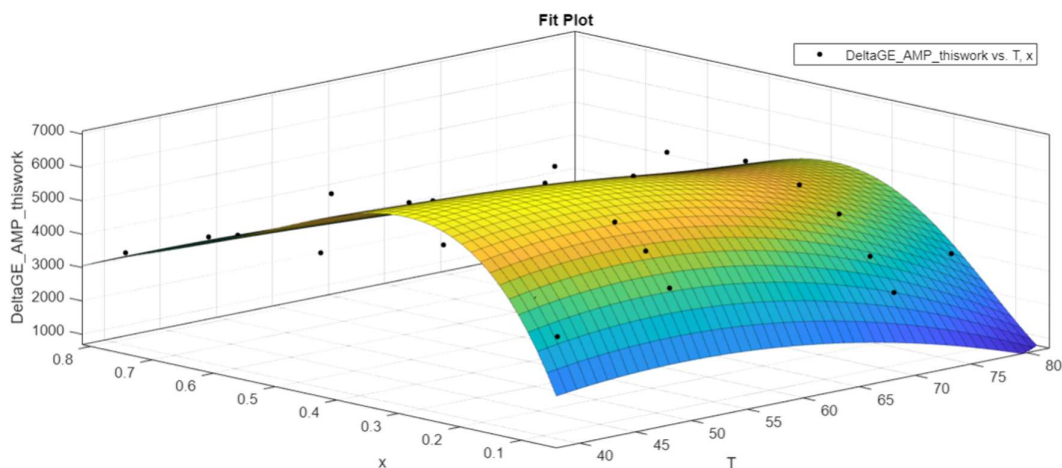
Figure 5.6:Fitted curve for aqueous AMP data using MATLAB (Eyring's viscosity model).

5.2.2 Arrhenius equation for modeling viscosity data

Arrhenius equation as described in equation 5.9 is well known to correlate the viscosity to temperature.

$$\mu = A_0 e^{Eav/RT} \qquad (5.9)$$

In this equation μ, A_0, R, and T are viscosity, a preexponential factor, gas constant, and temperature, respectively [14].

Guo et al. has suggested a model by using extended Arrhenius equation to study the viscosity of aqueous EAE solutions as described in equation 5.10 [15].

$$\ln(\eta) = \frac{m * w_1 + n}{RT} + pw_1 + q \qquad (5.10)$$

m, n, p, and q, in equation 5.10, are adjustable parameters for the extended Arrhenius equation.

5.2.2.1 Arrhenius equation for modeling aqueous MEA viscosity data

The viscosity in equation 5.10 is directly described using five coefficients, temperature, and weight fraction of the amine, making it a less complicated model than Eyring's viscosity model. By utilizing the aforementioned equation, the coefficients for the viscosity data were evaluated using MATLAB curve fitting software, and the results are presented in table 5.11 and fitted curve can be found in figure 5.7. This table also includes fitness quality measuring parameters.

Table 5.11: Calculated coefficients of Arrhenius equation viscosity model for aqueous MEA from 303.15 K up to 353.15 K

Coefficient	Value	Goodness of the fit
m	2.47E+04	R²=0.9828 AARD=9.87% AMD= 1.9391 $(m.Pa.s)$
n	9537	
p	-6.491	
q	-3.945	
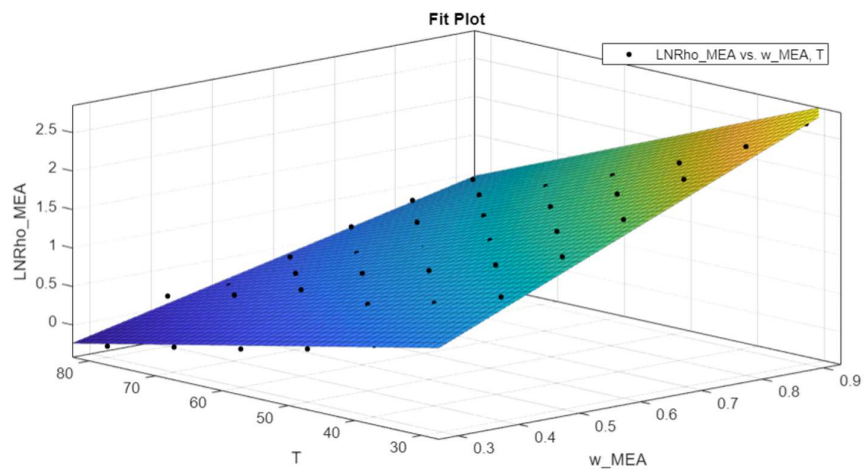
Figure 5.7: Fitted curve for aqueous MEA data using MATLAB (Arrhenius equation viscosity model).

5.2.2.2 Arrhenius equation for modeling aqueous AMP viscosity data

Table 5.12 includes the evaluated coefficient for the Arrhenius equation using MATLAB curve fitting for AMP plus water mixture with weight fraction from 30 up to 95 percent of AMP in the temperature range of 313.15 K up to 353.15 K. the fitting is also illustrated in figure 58.

Table 5.12: Calculated coefficients of Arrhenius equation viscosity model for aqueous MEA from 313.15 K up to 333.15 K

Coefficient	Value	Goodness of the fit
m	3.64E+04	R²=0.9975 AARD=3.776% AMD= 4.28 $(m.Pa.s)$
n	1.14E+04	
p	-9.351	
q	-5.005	
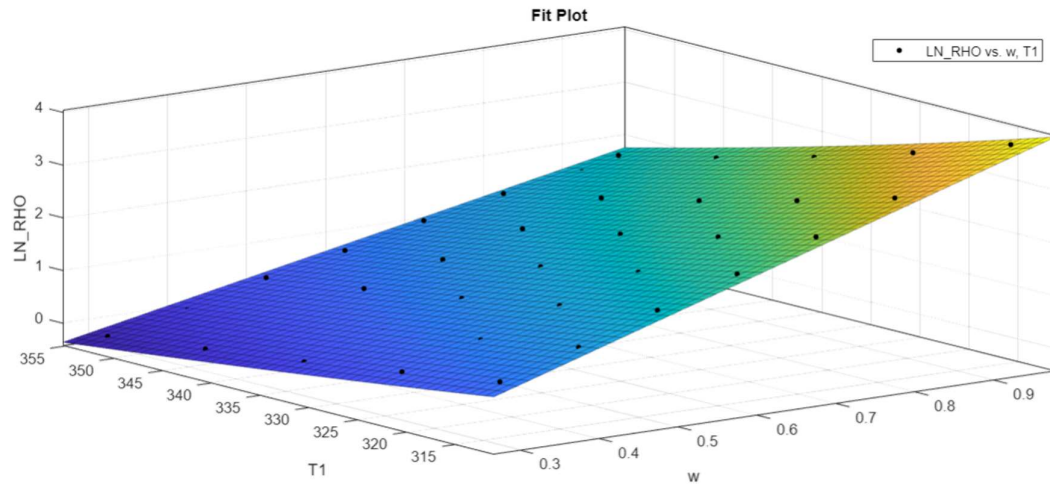
Figure 5.8: Fitted curve for aqueous AMP data using MATLAB (Arrhenius equation viscosity model).

6 Conclusion

6.1 Experimental data

In this section, we will provide a concise summary of the significant findings obtained during the experiment. Additionally, we will provide explanations for the various measurements that were taken.

6.1.1 Experimental data for Density

As described in section 4.1. density of MEA and AMP solutions were experimented and compared with selected resources which the summarized comparison between the data is tabulated in table 6.1.

Table 6.1: Measured density data overview

Amine	Number of data points	Mole fraction range	Temperature range (K)	AARD %		AMD (kg/m^3)	
MEA	48	0.068-1	303.15-353.15	S1	0.029%	S1	0.284
				S2	0.032%	S2	0.2843
AMP	51	0.079-1	313.15-353.15	0.222%		0.920	
S1 refers to Trine et al. [6].							
S2 refers to Karunarathne et al. [5].							

 A reliable experimental data is shown in both solutions, as indicated by the evaluated AARD and AMD in MEA measurement data. The slightly higher values observed in AMP can be attributed to two factors. Firstly, the experiment results were compared to a mathematical model proposed by Henni et al.[7], rather than their actual experimental data, which could lead to greater discrepancies in the data. As previously explained, the different mole fraction and temperature ranges made it impossible to compare the results of this study with theirs.

Secondly, the difference in accuracy of the measurement tools used could also be a contributing factor. Despite taking all necessary measures to ensure maximum accuracy in the experiment, errors in reading and testing procedures are an inevitable part of experimental work and can contribute to inaccuracies.

6.1.2 Experimental data for Viscosity

Regarding experiments done for measuring viscosity of the selected amines, the values compared with resources with same stick yards as in density section. This comparison is tabulated in table 6.2.

Table 6.2: Measured viscosity data overview

Amine	Number of data points	Mole fraction range	Temperature range (K)	AARD %		AMD ($mPa.s$)	
MEA	48	0.068-1	303.15-353.15	S1	6.07%	S1	0.415
				S2	1.093%	S2	0.642
AMP	51	0.079-1	313.15-353.15	5.186%		8.51	
S1 refers to Trine et al. [6].							
S2 refers to Karunarathne et al. [5].							

The results of the MEA evaluations show better accuracy compared to those of Karunarathne et al. This is expected because both studies used the same measurement method. As for the AMP density measurements, the higher deviations may be attributed to two factors. Firstly, the values used to compare the data in this study were derived from a model proposed by Henni et al., which naturally introduces some deviation from real data. Secondly, the measurement method used in this study differed from that used in previous research. Overall, these factors could account for the observed deviations.

However, the accuracy of the measured data for MEA suggests that the procedures used to measure viscosity were accurate enough, and thus the experimental data for AMP can also be considered accurate.

It's important to note that viscosity measurements are highly precise and sensitive procedures that are easily influenced by environmental factors such as air flow and vibration of surrounding objects. This could explain some of the differences observed.

6.2 Mathematical models

In this part of concluding section, we compare and evaluate the various models used to simulate our experimental findings. these models are assessed based on parameters such as AMD, AARD, and the number of coefficients required, which provide an indication of the ease of use of each model.

6.2.1 Density mathematical models

For both MEA and AMP solutions, Redlich-Kister polynomial (calculating excess molar volume) and Aronu model were suggested to model the experimental data and the result are shown in table 6.3.

Table 6.3: Comparison between different mathematical models for density data

Amine	Model	Number of Coefficient	R-squared	AARD	AMD (Kg/m^3)
MEA	Redlich-Kister	8	0.9925	0.047%	2.85

	Aronu	5	0.9741	0.1806%	5.46
AMP	Redlich-Kister	10	0.9624	0.158%	10.55
	Aronu	5	0.9753	0.123%	9.24

Table 6.3 demonstrates that, for MEA density data, the Redlich-Kister model provides slightly better and more accurate results than the Aronu model. However, the Redlich-Kister model requires a higher number of coefficients, making it more challenging to calculate.

In contrast, for AMP results, both the Redlich-Kister and Aronu models produce similar results, but the Aronu model is slightly more accurate. Additionally, the Aronu model is easier to use since it calculates the density directly, rather than the excess property. Thus, the Aronu model is the more convenient option for future use.

6.2.2 Viscosity mathematical models

Following the same procedure as density, two models, Eyring's viscosity model and the Arrhenius equation, were employed to illustrate the findings in mathematical form for modeling the viscosity data. The excess free energy of activation is calculated first, followed by the viscosity, in the first method, while the second model directly calculates the viscosity. Table 6.4 shows a comparison of these two models.

Table 6.4: Comparison between different mathematical models for viscosity data

Amine	Model	Number of Coefficient	R-squared	AARD	AMD $(m.Pa.s)$
MEA	Eyring's viscosity	9	0.9476	17.69%	4.347
	Arrhenius	4	0.9828	9.87%	1.9391
AMP	Eyring's viscosity	12	0.921	76.6%	43.013
	Arrhenius	4	0.9975	3.776%	4.28

The Arrhenius equation is a more reliable and easier-to-use model than the Eyring's viscosity model for both experimental datasets. The Arrhenius equation better describes the experimental findings, and requires fewer calculations than the Eyring's viscosity model. Despite employing higher degrees and more sentences for the calculation, the Eyring's viscosity model was still unable to accurately describe the data.

6.3 Future work

To further advance the findings of this study, potential areas for future research can be divided into two categories: expanding experimental investigations and advancing mathematical modeling. These avenues for exploration will be elaborated upon in the following sections.

6.3.1 expanding experimental investigations

the weak points in this work can be mentioned as follows:

- insufficient comparison for AMP data in both density and viscosity measurement.
- lack of measurement in high mole fractions for AMP solution.
- Unrepeated experiment for viscosity to increase accuracy.

To address these issues, the experiment should include high concentrated AMP solutions, and viscosity measurements should be repeated at least two more times to improve accuracy. However, preparing high concentrated AMP solutions can be challenging due to the mixture's high molar weight and the possibility of crystallization at room temperature, which can damage the instrument.

Regarding the insufficient comparison for AMP data, since there is not much report available for aqueous AMP solution, the only suggestion could be creating mole fractions of AMP plus water so that covers the available literature data.

Additionally, investigating the physical properties of mixtures of AMP and MEA can contribute to the development of carbon capture processes, as AMP is often used with other amines in this process. Finally, studying CO_2 loaded AMP solutions is a unique area of research due to the lack of available data.

6.3.2 Advancing mathematical modeling

To develop the models which can describe this works finding, one solution can be testing and evaluate other well-known models such as Jouyban-Acree model and Weiland model for viscosity.

References

[1]   B. Metz *et al.*, *IPCC special report on carbon dioxide capture and storage*, Cambridge England,New York, NY: Published for the Intergovernmental Panel on Climate Change, Cambridge University Press, 2005.

[2]   J. R. Couper, W. R. Penney, J. R. Fair, and P. J. R. Fair, *Chemical Process Equipment : Selection and Design*. Oxford, UNITED STATES: Elsevier Science & Technology, 2012.

[3]   C.-H. Yu, C.-H. Huang, and C.-S. Tan, "A Review of CO2 Capture by Absorption and Adsorption," *Aerosol and air quality research,* vol. 12, no. 5, pp. 745-769, 2012, doi: 10.4209/aaqr.2012.05.0132.

[4]   Y. Wu, J. Xu, K. Mumford, G. W. Stevens, W. Fei, and Y. Wang, "Recent advances in carbon dioxide capture and utilization with amines and ionic liquids," *Green Chemical Engineering,* vol. 1, no. 1, pp. 16-32, 2020, doi: 10.1016/j.gce.2020.09.005.

[5]   S. S. Karunarathne, D.-A. Eimer, and L. E. Øi, "Density, viscosity and free energy of activation for viscous flow of monoethanol amine (1) + H2O (2) + CO2 (3) mixtures," 2020, doi: https://doi.org/10.3390/fluids5010013.

[6]   T. G. Amundsen, L. E. Oi, and D. A. Eimer, "Density and Viscosity of Monoethanolamine plus Water plus Carbon Dioxide from (25 to 80) degrees C," *Journal of chemical and engineering data,* vol. 54, no. 11, pp. 3096-3100, 2009, doi: 10.1021/je900188m.

[7]   A. Henni, J. J. Hromek, P. Tontiwachwuthikul, and A. Chakma, "Volumetric Properties and Viscosities for Aqueous AMP Solutions from 25 °C to 70 °C," *J. Chem. Eng. Data,* vol. 48, no. 3, pp. 551-556, 2003, doi: 10.1021/je0201119.

[8]   C. C. Chemistry. "chemical information." https://commonchemistry.cas.org (accessed 7 May 2023, 2023).

[9]   W. M. Haynes, D. R. Lide, and T. J. Bruno, *CRC handbook of chemistry and physics : a ready-reference book of chemical and physical data*, Ninety-seven edition. ed. Boca Raton, Florida,London, England,New York: CRC Press, 2017.

[10]   R. E. Sonntag, G. J. Van Wylen, and C. Borgnakke, *Fundamentals of thermodynamics*, 6th ed. New York: Wiley, 2003.

[11]   O. Redlich and A. T. Kister, "Algebraic Representation of Thermodynamic Properties and the Classification of Solutions," *Industrial and engineering chemistry,* vol. 40, no. 2, pp. 345-348, 1948, doi: 10.1021/ie50458a036.

[12]   U. E. Aronu, A. Hartono, and H. F. Svendsen, "Density, viscosity, and N2O solubility of aqueous amino acid salt and amine amino acid salt solutions," *The Journal of chemical thermodynamics,* vol. 45, no. 1, pp. 90-99, 2012, doi: 10.1016/j.jct.2011.09.012.

[13]   J. Han, J. Jin, D. A. Eimer, and M. C. Melaaen, "Density of Water (1) + Monoethanolamine (2) + CO2 (3) from (298.15 to 413.15) K and Surface Tension of

Water (1) + Monoethanolamine (2) from (303.15 to 333.15) K," *J. Chem. Eng. Data,* vol. 57, no. 4, pp. 1095-1103, 2012, doi: 10.1021/je2010038.

[14]   A. Messaâdi *et al.*, "A New Equation Relating the Viscosity Arrhenius Temperature and the Activation Energy for Some Newtonian Classical Solvents," *Journal of chemistry,* vol. 2015, pp. 1-12, 2015, doi: 10.1155/2015/163262.

[15]   P. Yang, C. Liu, Q. Guo, and Y. Liu, "Variation of activation energy determined by a modified Arrhenius approach: Roles of dynamic recrystallization on the hot deformation of Ni-based superalloy," *Journal of materials science & technology,* vol. 72, pp. 162-171, 2021, doi: 10.1016/j.jmst.2020.09.024.

Appendices

Appendix A: Coefficients of polynomial offered by Henni et al. for AMP density and viscosity.

Appendix B: Details of measurement driven from the rheometer device.

Appendix C: Details of calculations and MATLAB code for modeling density data.

Appendix D: Details of calculations and MATLAB code for modeling viscosity data.

Appendix A

Table A.1: Coefficients of the Polynomial and the Standard Deviations offered by Henni et al. for the aqueous AMP Solutions density at Various Temperatures.

T	a_0	a_1	a_2	a_3	a_4	a_5	Deviation
25	0.99664	0.05597	-0.71889	1.442	-1.26103	0.41692	0.0005
30	0.99578	0.00862	-0.42705	0.64412	-0.29992	0	0.0006
40	0.99203	-0.01389	-0.46712	0.99755	-0.87903	0.29021	0.0004
50	0.98794	-0.05063	-0.35228	0.83676	-0.77954	0.26908	0.0003
60	0.98311	-0.08256	-0.24621	0.6674	-0.65025	0.23148	0.0003
70	0.97819	-0.13097	0.00477	0.08077	-0.03857	0	0.0004

Table A.2: Coefficients of the Polynomial offered by Henni et al. for the aqueous AMP Solutions viscosity at Various Temperatures.

T	a_0	a_1	a_2	a_3	a_4	a_5
25	22.627	-67.322	137.11	-143.375	56.582	0.07
30	21.047	-61.664	125.419	-131.883	52.368	0.07
40	18.576	-45.781	74.028	-64.246	21.722	0.03
50	16.843	-41.624	66.893	-57.753	19.475	0.03
60	15.146	-36.545	56.947	-48.085	15.973	0.01
70	14.465	-38.175	63.103	-54.56	18.263	0.03

Appendix B: Details of measurement driven from the rheometer device.
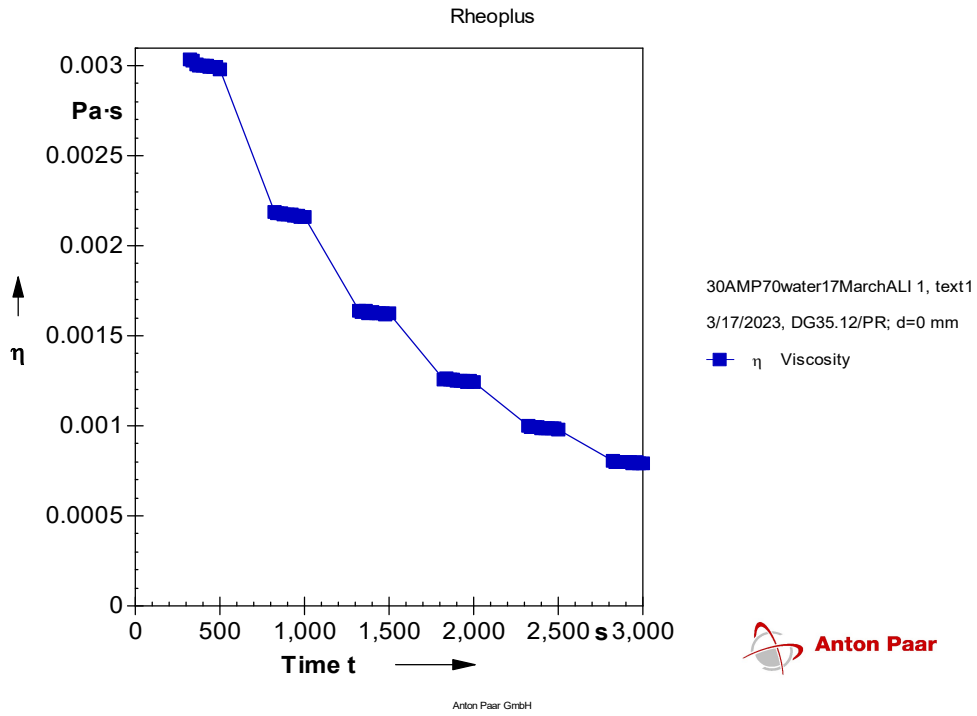
Figure B.1: Exported curve for 30% weight AMP by rheometer device.
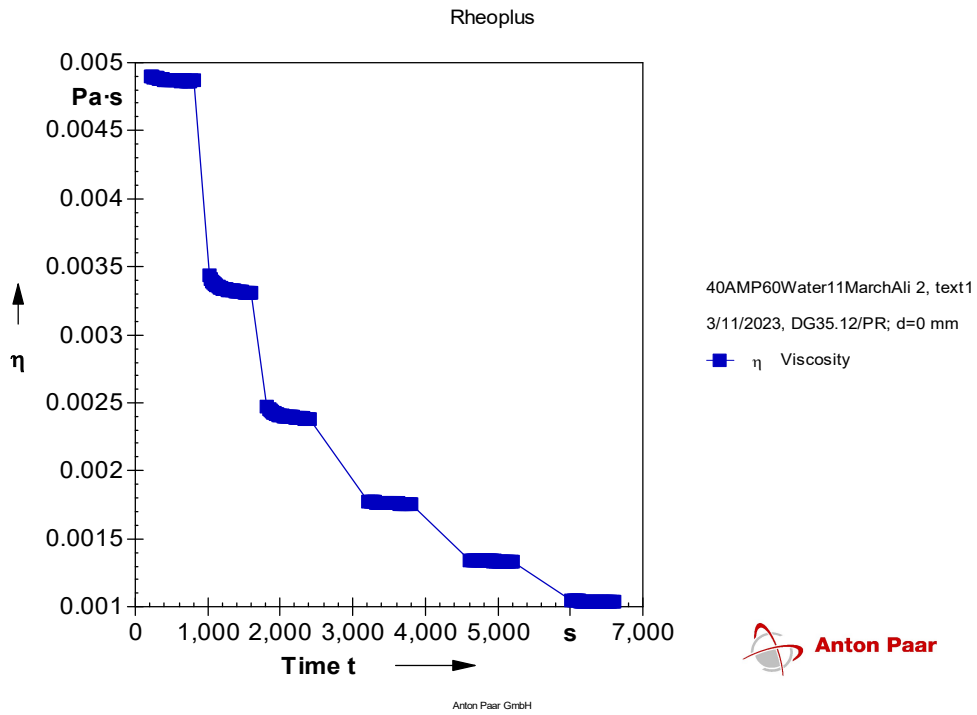
Figure B.2: Exported curve for 40% weight AMP by rheometer device.
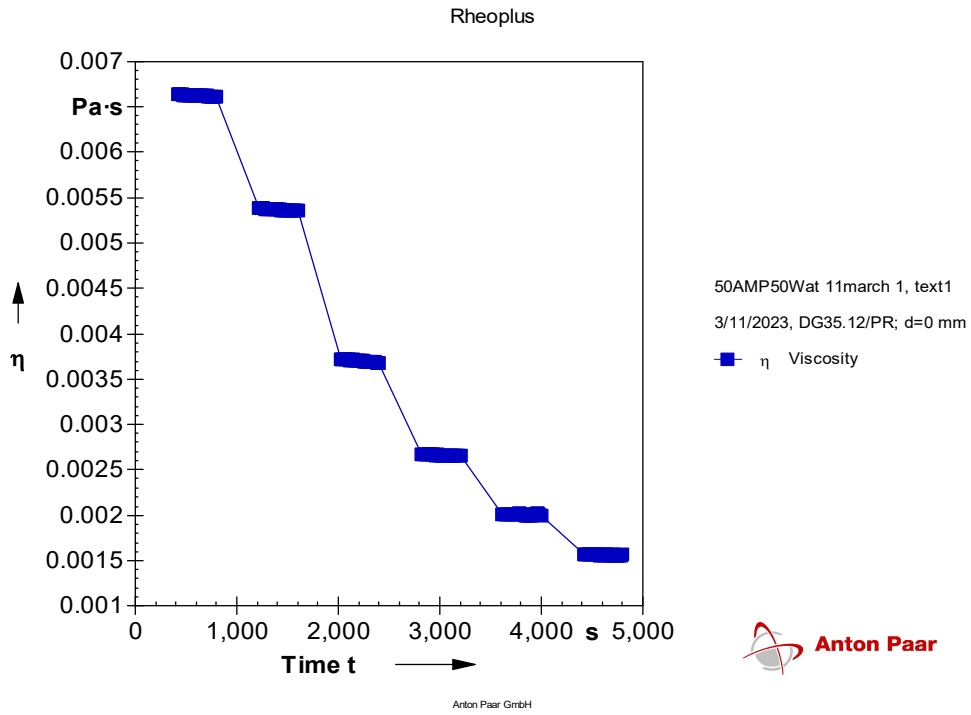
Figure B.3: Exported curve for 50% weight AMP by rheometer device.
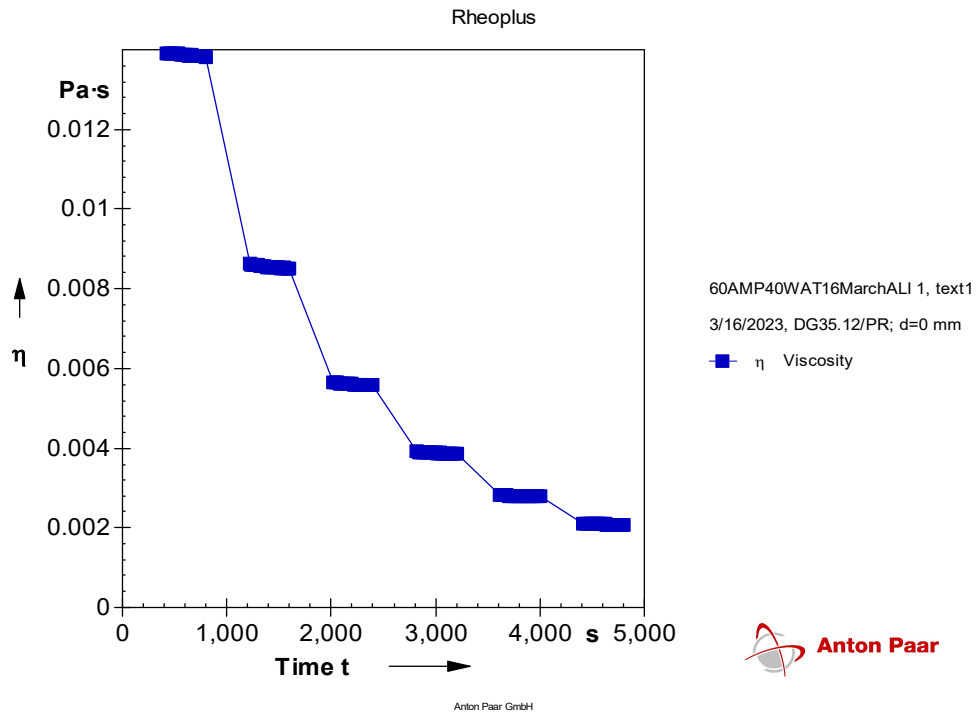
Figure B.4: Exported curve for 60% weight AMP by rheometer device.
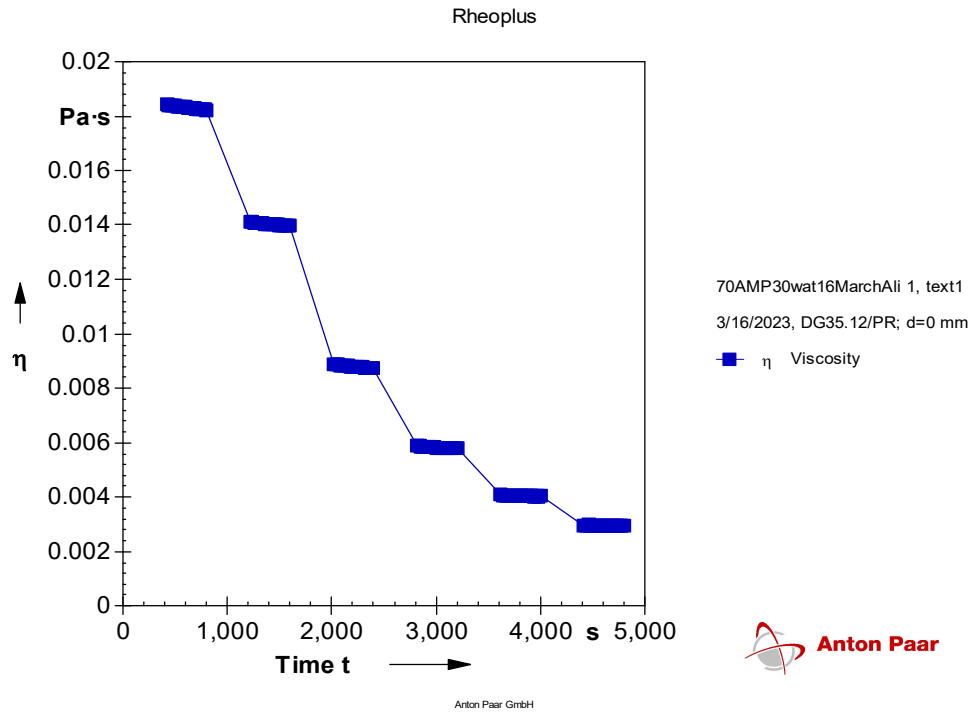
Figure B.5: Exported curve for 70% weight AMP by rheometer device.
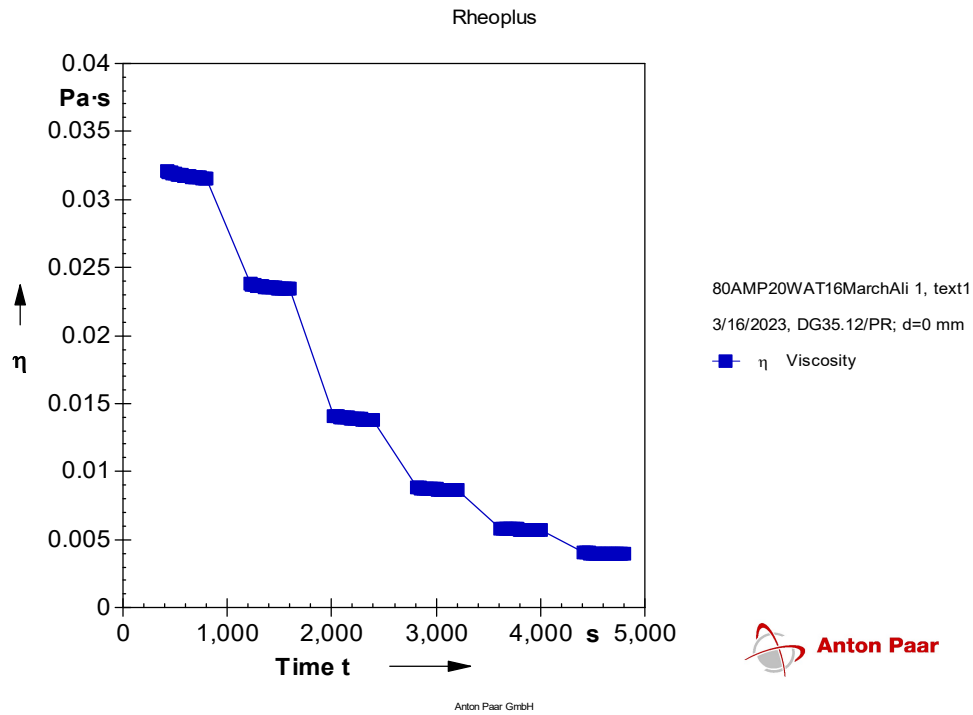
Figure B.6: Exported curve for 80% weight AMP by rheometer device.
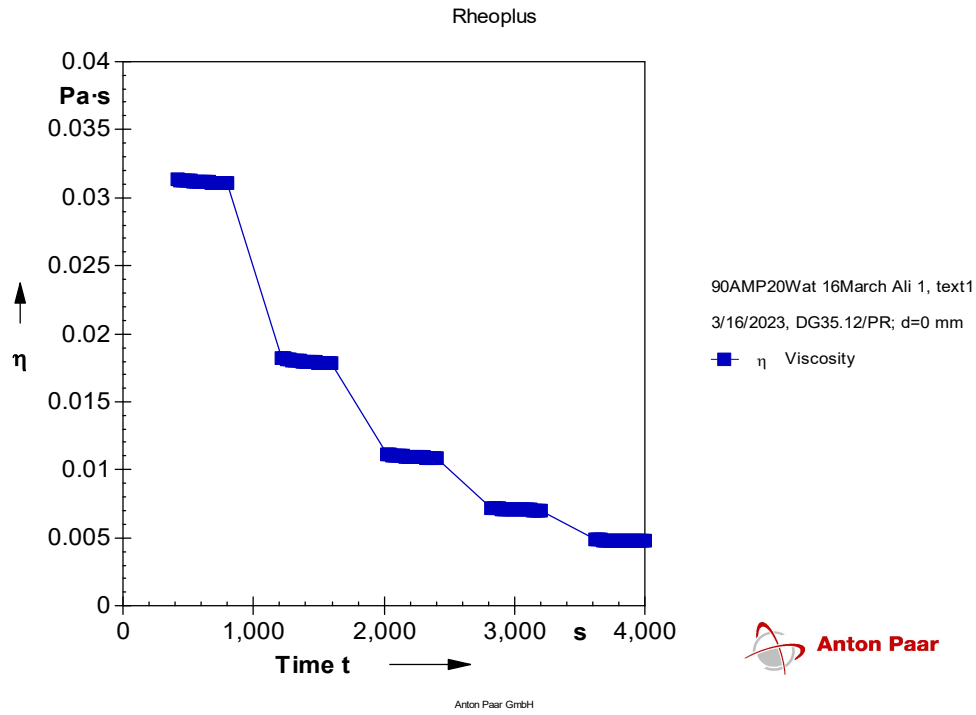
Figure B.7: Exported curve for 90% weight AMP by rheometer device.
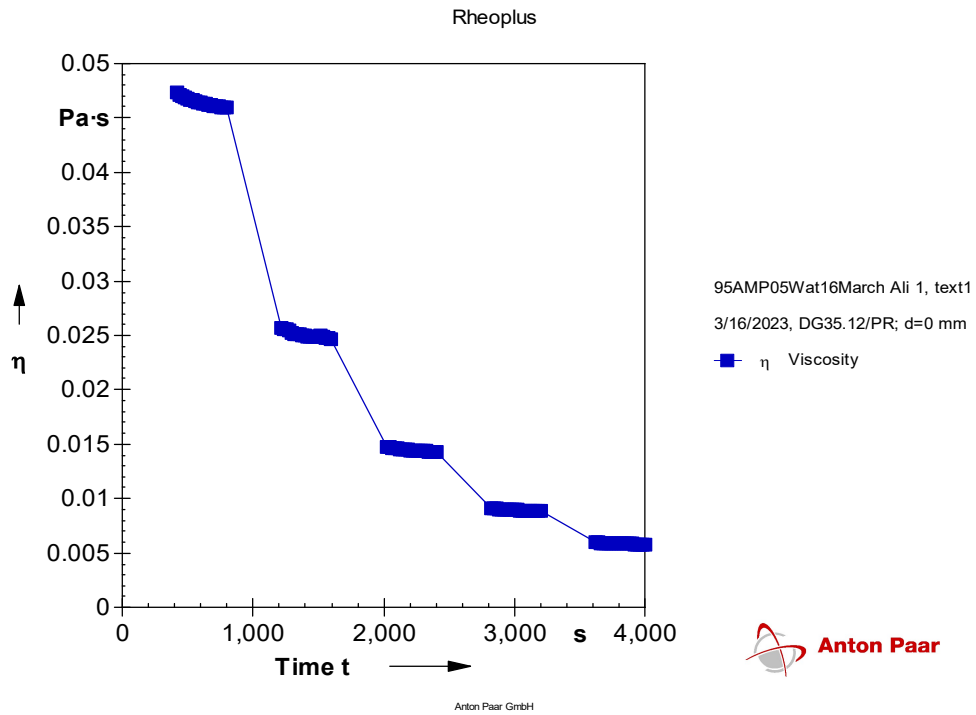
Figure B.8: Exported curve for 95% weight AMP by rheometer device.
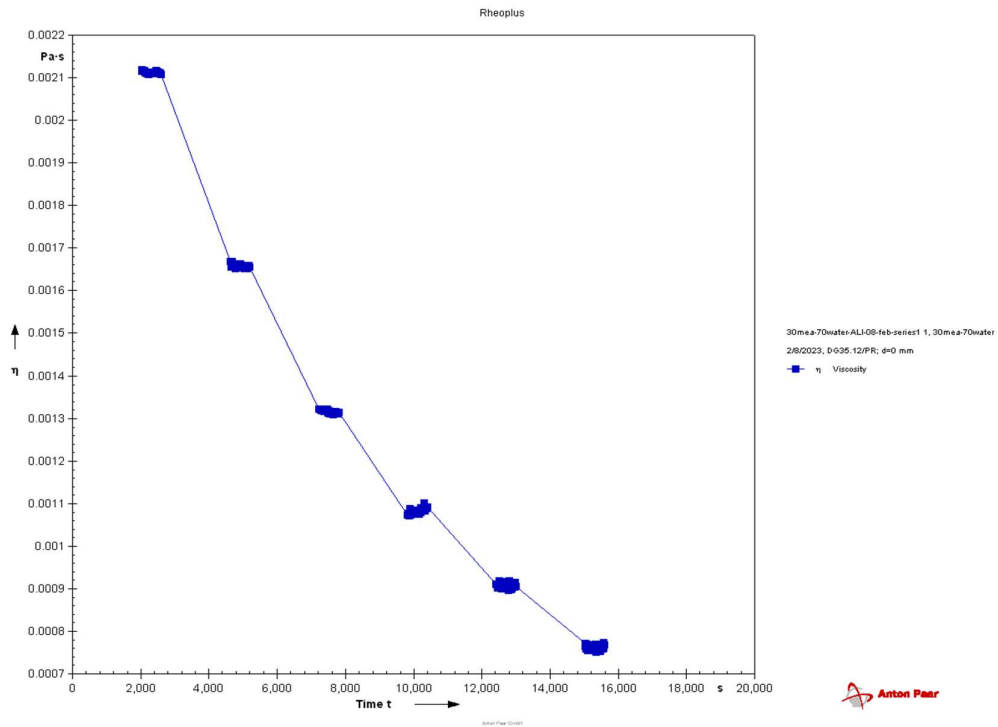
Figure B.9: Exported curve for 30% weight MEA by rheometer device.
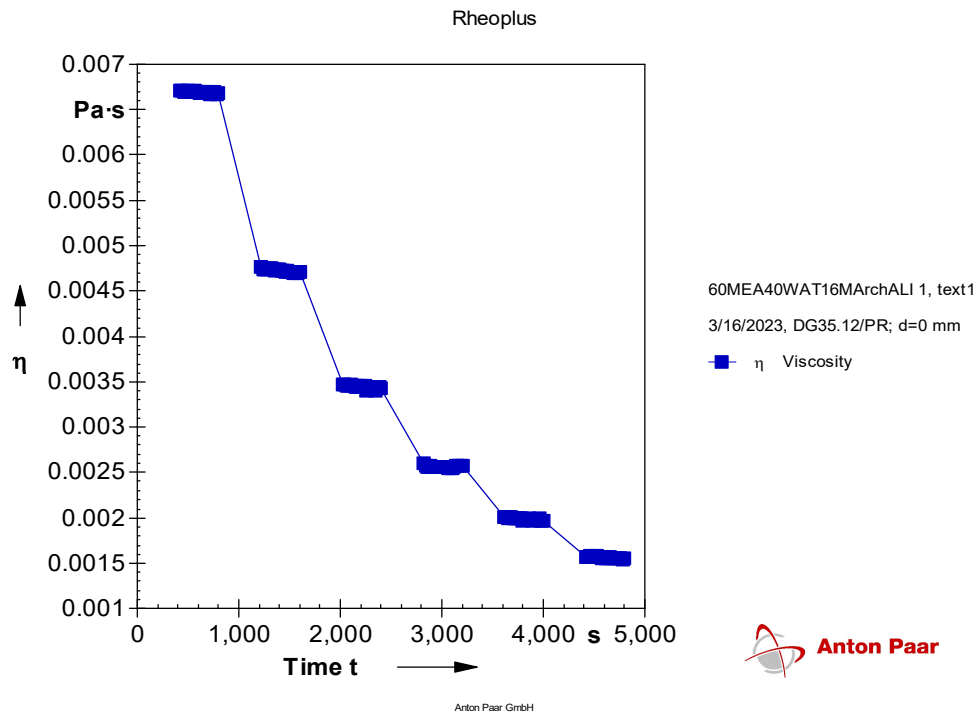
Figure B.10: Exported curve for 60% weight MEA by rheometer device.
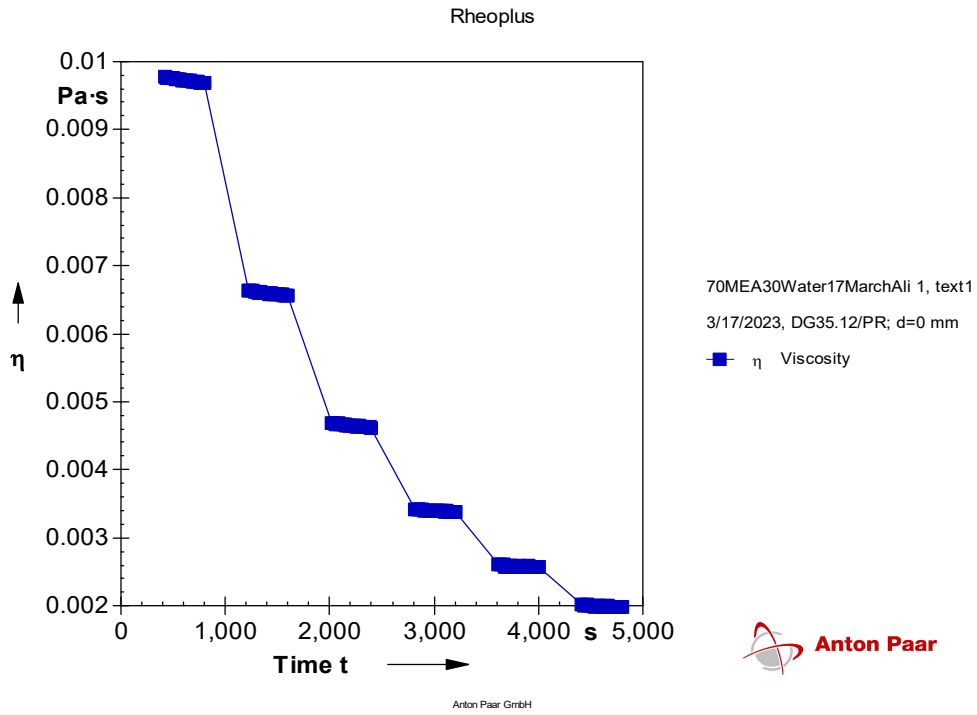
Figure B.11: Exported curve for 70% weight MEA by rheometer device.
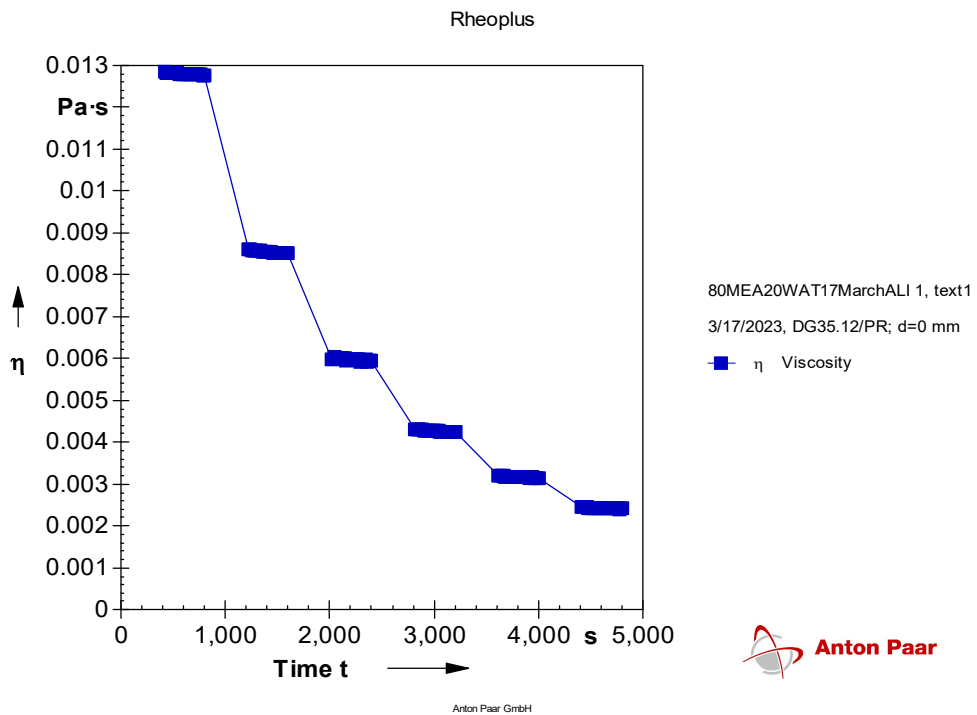
Figure B.12: Exported curve for 80% weight MEA by rheometer device.
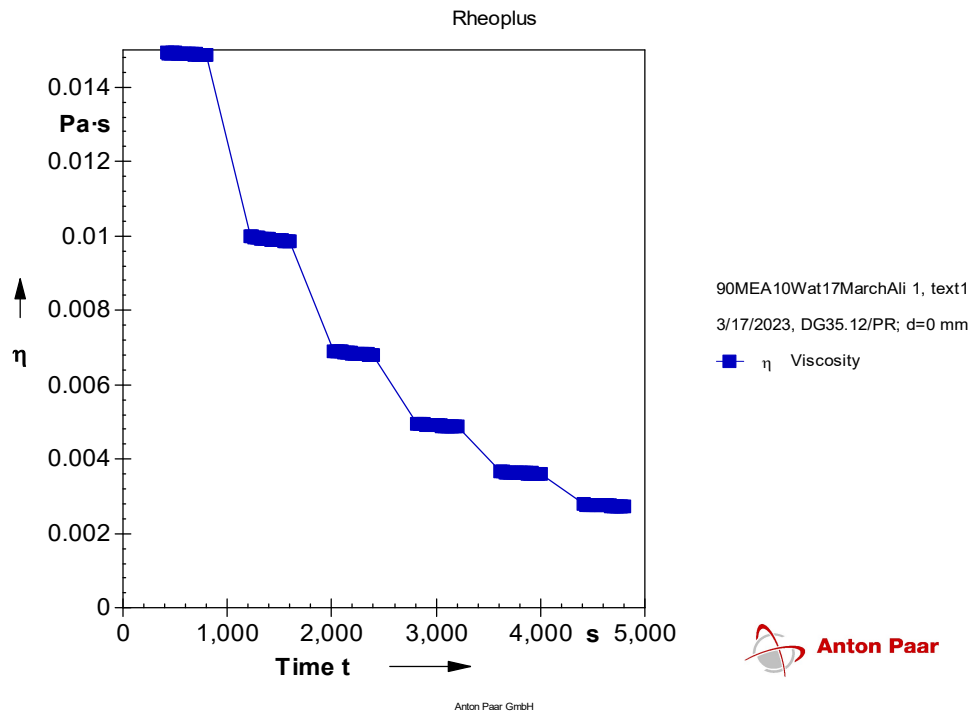
Figure B.13: Exported curve for 90% weight MEA by rheometer device.

Appendix C: Details of calculations and MATLAB code for modeling density data.

Table C.1: detailed calculation for modeling MEA density data

T (°C)	x_{MEA}	M_{mix}	ρ_{mix}	v_{mix}	v_{ideal}	v^E	v^E Recalculated	v_{mix} Recalculated	ρ_{mix} Recalculated
30	0.1123	0.0229	1008.2600	2.27E-05	2.29E-05	-1.98E-07	-1.90E-07	2.27E-05	1007.909
30	0.1643	0.0251	1013.4200	2.48E-05	2.51E-05	-3.11E-07	-2.94E-07	2.48E-05	1012.732
30	0.2277	0.0278	1018.1100	2.73E-05	2.78E-05	-4.35E-07	-4.13E-07	2.73E-05	1017.278
30	0.3068	0.0312	1021.3700	3.06E-05	3.11E-05	-5.46E-07	-5.29E-07	3.06E-05	1020.809
30	0.4070	0.0355	1022.7000	3.48E-05	3.54E-05	-6.21E-07	-6.08E-07	3.48E-05	1022.325
30	0.5411	0.0413	1020.9900	4.05E-05	4.11E-05	-6.00E-07	-5.95E-07	4.05E-05	1020.868
30	0.7260	0.0493	1016.1100	4.85E-05	4.89E-05	-4.20E-07	-4.27E-07	4.85E-05	1016.263
30	1.0000	0.0611	1008.7100	6.06E-05	6.06E-05	0.00E+00	0.00E+00	6.06E-05	1008.710
40	0.1123	0.0229	1003.7700	2.28E-05	2.29E-05	-8.58E-08	-1.12E-07	2.27E-05	1004.930
40	0.1643	0.0251	1007.8300	2.49E-05	2.51E-05	-1.95E-07	-2.13E-07	2.49E-05	1008.549
40	0.2277	0.0278	1011.8100	2.75E-05	2.78E-05	-3.24E-07	-3.37E-07	2.75E-05	1012.282
40	0.3068	0.0312	1014.6400	3.08E-05	3.12E-05	-4.50E-07	-4.66E-07	3.08E-05	1015.151
40	0.4070	0.0355	1015.4700	3.50E-05	3.55E-05	-5.41E-07	-5.55E-07	3.50E-05	1015.895
40	0.5411	0.0413	1013.4700	4.08E-05	4.13E-05	-5.48E-07	-5.48E-07	4.08E-05	1013.471
40	0.7260	0.0493	1008.4300	4.89E-05	4.93E-05	-4.11E-07	-4.03E-07	4.89E-05	1008.275
40	1.0000	0.0611	1000.0300	6.11E-05	6.11E-05	0.00E+00	0.00E+00	6.11E-05	1000.030
50	0.1123	0.0229	998.0400	2.29E-05	2.29E-05	-1.42E-08	-3.45E-08	2.29E-05	998.924
50	0.1643	0.0251	1001.9100	2.50E-05	2.52E-05	-1.32E-07	-1.31E-07	2.50E-05	1001.854
50	0.2277	0.0278	1005.7300	2.77E-05	2.79E-05	-2.74E-07	-2.62E-07	2.77E-05	1005.290
50	0.3068	0.0312	1007.7300	3.10E-05	3.14E-05	-3.93E-07	-4.02E-07	3.10E-05	1008.022
50	0.4070	0.0355	1008.1200	3.53E-05	3.57E-05	-4.89E-07	-5.03E-07	3.52E-05	1008.530
50	0.5411	0.0413	1005.8700	4.11E-05	4.16E-05	-5.09E-07	-5.01E-07	4.11E-05	1005.690
50	0.7260	0.0493	1000.4200	4.93E-05	4.96E-05	-3.78E-07	-3.79E-07	4.93E-05	1000.440
50	1.0000	0.0611	992.0300	6.16E-05	6.16E-05	0.00E+00	0.00E+00	6.16E-05	992.030
60	0.1123	0.0229	992.2300	2.30E-05	2.30E-05	5.22E-08	4.31E-08	2.30E-05	992.625
60	0.1643	0.0251	995.6500	2.52E-05	2.53E-05	-6.80E-08	-4.91E-08	2.52E-05	994.905
60	0.2277	0.0278	998.6200	2.79E-05	2.81E-05	-2.01E-07	-1.86E-07	2.79E-05	998.073
60	0.3068	0.0312	999.8200	3.12E-05	3.15E-05	-3.11E-07	-3.39E-07	3.12E-05	1000.693
60	0.4070	0.0355	1000.6000	3.55E-05	3.60E-05	-4.37E-07	-4.51E-07	3.55E-05	1000.996
60	0.5411	0.0413	998.0400	4.14E-05	4.19E-05	-4.65E-07	-4.54E-07	4.14E-05	997.779
60	0.7260	0.0493	992.4300	4.97E-05	5.00E-05	-3.52E-07	-3.55E-07	4.97E-05	992.501
60	1.0000	0.0611	983.9600	6.21E-05	6.21E-05	0.00E+00	0.00E+00	6.21E-05	983.960
70	0.1123	0.0229	985.6900	2.32E-05	2.31E-05	1.31E-07	1.21E-07	2.32E-05	986.118
70	0.1643	0.0251	989.0000	2.54E-05	2.54E-05	1.48E-09	3.26E-08	2.54E-05	987.788
70	0.2277	0.0278	991.6200	2.81E-05	2.82E-05	-1.36E-07	-1.10E-07	2.81E-05	990.719
70	0.3068	0.0312	992.5200	3.15E-05	3.17E-05	-2.52E-07	-2.75E-07	3.14E-05	993.255
70	0.4070	0.0355	992.6000	3.58E-05	3.62E-05	-3.70E-07	-3.98E-07	3.58E-05	993.383
70	0.5411	0.0413	990.1800	4.17E-05	4.21E-05	-4.22E-07	-4.08E-07	4.17E-05	989.827
70	0.7260	0.0493	984.4500	5.01E-05	5.04E-05	-3.26E-07	-3.31E-07	5.01E-05	984.551

70	1.0000	0.0611	975.9100	6.26E-05	6.26E-05	0.00E+00	0.00E+00	6.26E-05	975.910
80	0.1123	0.0229	976.5600	2.34E-05	2.31E-05	2.66E-07	1.98E-07	2.33E-05	979.406
80	0.1643	0.0251	982.0200	2.56E-05	2.55E-05	7.41E-08	1.14E-07	2.56E-05	980.477
80	0.2277	0.0278	984.2500	2.83E-05	2.83E-05	-6.57E-08	-3.46E-08	2.83E-05	983.170
80	0.3068	0.0312	985.4800	3.17E-05	3.19E-05	-2.07E-07	-2.12E-07	3.17E-05	985.616
80	0.4070	0.0355	985.5300	3.61E-05	3.64E-05	-3.44E-07	-3.46E-07	3.61E-05	985.569
80	0.5411	0.0413	982.1200	4.21E-05	4.24E-05	-3.79E-07	-3.61E-07	4.21E-05	981.683
80	0.7260	0.0493	976.3000	5.05E-05	5.08E-05	-3.02E-07	-3.07E-07	5.05E-05	976.406
80	1.0000	0.0611	967.6700	6.31E-05	6.31E-05	0.00E+00	0.00E+00	6.31E-05	967.670

Table C.2: detailed calculation for modeling MEA density data

T (°C)	x_{MEA}	M_{mix}	ρ_{mix}	v_{mix}	v_{ideal}	v^E	v^E Recalculated	v_{mix} Recalculated	ρ_{mix} Recalculated
40	0.08	0.02370	9.88E+02	2.40E-05	2.43E-05	-3.45E-07	-4.66E-07	2.39E-05	993.382
40	0.119	0.02648	9.86E+02	2.69E-05	2.74E-05	-5.52E-07	-5.62E-07	2.68E-05	986.386
40	0.168	0.02996	9.81E+02	3.05E-05	3.13E-05	-7.35E-07	-6.84E-07	3.06E-05	979.539
40	0.233	0.03459	9.74E+02	3.55E-05	3.64E-05	-8.93E-07	-8.79E-07	3.55E-05	973.615
40	0.321	0.04085	9.64E+02	4.24E-05	4.33E-05	-9.94E-07	-1.10E-06	4.22E-05	966.782
40	0.447	0.04981	9.52E+02	5.23E-05	5.33E-05	-9.94E-07	-9.53E-07	5.23E-05	951.643
40	0.645	0.06389	9.30E+02	6.87E-05	6.89E-05	-1.88E-07	-2.38E-07	6.87E-05	930.275
40	0.7797	0.07347	9.38E+02	7.83E-05	7.95E-05	-1.20E-06	-1.21E-06	7.83E-05	937.937
40	1	0.08914	9.20E+02	9.69E-05	9.69E-05	0.00E+00	0.00E+00	9.69E-05	919.600
50	0.08	0.02370	9.82E+02	2.41E-05	2.44E-05	-2.77E-07	-3.39E-07	2.41E-05	984.729
50	0.119	0.02648	9.79E+02	2.71E-05	2.75E-05	-4.73E-07	-4.37E-07	2.71E-05	977.395
50	0.168	0.02996	9.73E+02	3.08E-05	3.14E-05	-6.57E-07	-5.80E-07	3.09E-05	970.863
50	0.233	0.03459	9.66E+02	3.58E-05	3.66E-05	-8.25E-07	-8.07E-07	3.58E-05	965.318
50	0.321	0.04085	9.56E+02	4.27E-05	4.37E-05	-9.52E-07	-1.05E-06	4.26E-05	958.317
50	0.447	0.04981	9.44E+02	5.28E-05	5.37E-05	-9.80E-07	-8.91E-07	5.28E-05	942.510
50	0.645	0.06389	9.21E+02	6.94E-05	6.96E-05	-2.02E-07	-2.11E-07	6.93E-05	921.316
50	0.7797	0.07347	9.29E+02	7.90E-05	8.03E-05	-1.27E-06	-1.23E-06	7.91E-05	928.995
50	1	0.08914	9.10E+02	9.79E-05	9.79E-05	0.00E+00	0.00E+00	9.79E-05	910.300
60	0.08	0.02370	9.75E+02	2.43E-05	2.45E-05	-1.86E-07	-2.13E-07	2.43E-05	976.077
60	0.119	0.02648	9.71E+02	2.73E-05	2.77E-05	-3.84E-07	-3.12E-07	2.73E-05	968.510
60	0.168	0.02996	9.65E+02	3.10E-05	3.16E-05	-5.71E-07	-4.77E-07	3.11E-05	962.371
60	0.233	0.03459	9.58E+02	3.61E-05	3.69E-05	-7.44E-07	-7.36E-07	3.61E-05	957.280
60	0.321	0.04085	9.48E+02	4.31E-05	4.40E-05	-8.85E-07	-9.94E-07	4.30E-05	950.202
60	0.447	0.04981	9.36E+02	5.32E-05	5.42E-05	-9.29E-07	-8.29E-07	5.33E-05	933.829
60	0.645	0.06389	9.13E+02	7.00E-05	7.02E-05	-1.70E-07	-1.83E-07	7.00E-05	912.874
60	0.7797	0.07347	9.21E+02	7.98E-05	8.11E-05	-1.29E-06	-1.25E-06	7.98E-05	920.610
60	1	0.08914	9.02E+02	9.89E-05	9.89E-05	0.00E+00	0.00E+00	9.89E-05	901.600
70	0.08	0.02370	9.63E+02	2.46E-05	2.46E-05	2.00E-08	-8.62E-08	2.45E-05	967.275
70	0.119	0.02648	9.63E+02	2.75E-05	2.78E-05	-2.95E-07	-1.86E-07	2.76E-05	959.503
70	0.168	0.02996	9.57E+02	3.13E-05	3.18E-05	-4.76E-07	-3.73E-07	3.14E-05	953.762

70	0.233	0.03459	9.49E+02	3.64E-05	3.71E-05	-6.60E-07	-6.65E-07	3.64E-05	949.130
70	0.321	0.04085	9.39E+02	4.35E-05	4.43E-05	-8.12E-07	-9.41E-07	4.34E-05	941.996
70	0.447	0.04981	9.27E+02	5.37E-05	5.46E-05	-8.71E-07	-7.66E-07	5.38E-05	925.101
70	0.645	0.06389	9.04E+02	7.07E-05	7.08E-05	-1.16E-07	-1.56E-07	7.06E-05	904.402
70	0.7797	0.07347	9.12E+02	8.05E-05	8.18E-05	-1.28E-06	-1.27E-06	8.05E-05	912.195
70	1	0.08914	8.93E+02	9.98E-05	9.98E-05	0.00E+00	0.00E+00	9.98E-05	892.900
80	0.08	0.02370	9.48E+02	2.50E-05	2.47E-05	3.16E-07	4.03E-08	2.47E-05	958.353
80	0.119	0.02648	9.54E+02	2.77E-05	2.79E-05	-1.75E-07	-6.09E-08	2.79E-05	950.385
80	0.168	0.02996	9.48E+02	3.16E-05	3.20E-05	-3.69E-07	-2.70E-07	3.17E-05	945.027
80	0.233	0.03459	9.40E+02	3.68E-05	3.74E-05	-5.69E-07	-5.94E-07	3.68E-05	940.835
80	0.321	0.04085	9.30E+02	4.39E-05	4.46E-05	-7.31E-07	-8.89E-07	4.37E-05	933.649
80	0.447	0.04981	9.18E+02	5.43E-05	5.51E-05	-8.07E-07	-7.04E-07	5.44E-05	916.258
80	0.645	0.06389	8.95E+02	7.14E-05	7.14E-05	-6.29E-08	-1.28E-07	7.13E-05	895.817
80	0.7797	0.07347	9.04E+02	8.13E-05	8.26E-05	-1.30E-06	-1.29E-06	8.13E-05	903.657
80	1	0.08914	8.84E+02	1.01E-04	1.01E-04	0.00E+00	0.00E+00	1.01E-04	884.100

Sample MATLAB code used to fit AMP density data to a Redlich-Kister polynomial

```
CREATEFIT(T_AMP,X_AMP,VE_AMP)
%  Create a fit.
%
%  Data for 'untitled fit 1' fit:
%      X Input: T_AMP
%      Y Input: x_AMP
%      Z Output: VE_AMP
%  Output:
%      fitresult : a fit object representing the fit.
%      gof : structure with goodness-of fit info.
%
%  See also FIT, CFIT, SFIT.

%  Auto-generated by MATLAB on 30-Apr-2023 15:13:43


%% Fit: 'untitled fit 1'.
[xData, yData, zData] = prepareSurfaceData( T_AMP, x_AMP, VE_AMP );

% Set up fittype and options.
ft = fittype( '[(a00+a01*(T_AMP))+(a10+a11*(T_AMP))*(1-2*x_AMP)+(a20+a21*(T_AMP))*(1-
2*x_AMP)^2+(a30+a31*(T_AMP))*(1-2*x_AMP)^3+(a40+a41*(T_AMP))*(1-2*x_AMP)^4]*x_AMP*(1-
x_AMP)', 'independent', {'T_AMP', 'x_AMP'}, 'dependent', 'VE_AMP' );
opts = fitoptions( 'Method', 'NonlinearLeastSquares' );
opts.Display = 'Off';
opts.StartPoint = [0.706046088019609 0.0318328463774207 0.27692298496089
0.0461713906311539 0.0971317812358475 0.823457828327293 0.694828622975817
0.317099480060861 0.950222048838355 0.0344460805029088];

% Fit model to data.
[fitresult, gof] = fit( [xData, yData], zData, ft, opts );

% Plot fit with data.
figure( 'Name', 'untitled fit 1' );
h = plot( fitresult, [xData, yData], zData );
legend( h, 'untitled fit 1', 'VE_AMP vs. T_AMP, x_AMP', 'Location', 'NorthEast',
'Interpreter', 'none' );
% Label axes
xlabel( 'T_AMP', 'Interpreter', 'none' );
ylabel( 'x_AMP', 'Interpreter', 'none' );
zlabel( 'VE_AMP', 'Interpreter', 'none' );
grid on
```

Sample MATLAB code used to fit AMP density data to Aronu equation

```matlab
function [fitresult, gof] = createFit(x_AMP_AR, T_AMP_AR, RH_AMP)
%CREATEFIT(X_AMP_AR,T_AMP_AR,RH_AMP)
%  Create a fit.
%
%  Data for 'untitled fit 1' fit:
%      X Input: x_AMP_AR
%      Y Input: T_AMP_AR
%      Z Output: RH_AMP
%  Output:
%      fitresult : a fit object representing the fit.
%      gof : structure with goodness-of fit info.
%
%  See also FIT, CFIT, SFIT.

%  Auto-generated by MATLAB on 30-Apr-2023 15:19:00


%% Fit: 'untitled fit 1'.
[xData, yData, zData] = prepareSurfaceData( x_AMP_AR, T_AMP_AR, RH_AMP );

% Set up fittype and options.
ft = fittype( '(k1+((k2*(1-
x_AMP_AR))/T_AMP_AR))*exp((k3/T_AMP_AR)+(k4*x_AMP_AR/T_AMP_AR)+(k5*((x_AMP_AR/T_AMP_A
R)^2)))', 'independent', {'x_AMP_AR', 'T_AMP_AR'}, 'dependent', 'z' );
opts = fitoptions( 'Method', 'NonlinearLeastSquares' );
opts.Display = 'Off';
opts.StartPoint = [0.706046088019609 0.0318328463774207 0.27692298496089
0.0461713906311539 0.0971317812358475];

% Fit model to data.
[fitresult, gof] = fit( [xData, yData], zData, ft, opts );

% Plot fit with data.
figure( 'Name', 'untitled fit 1' );
h = plot( fitresult, [xData, yData], zData );
legend( h, 'untitled fit 1', 'RH_AMP vs. x_AMP_AR, T_AMP_AR', 'Location',
'NorthEast', 'Interpreter', 'none' );
% Label axes
xlabel( 'x_AMP_AR', 'Interpreter', 'none' );
ylabel( 'T_AMP_AR', 'Interpreter', 'none' );
zlabel( 'RH_AMP', 'Interpreter', 'none' );
grid on
```

Appendix D: Details of calculations and MATLAB code for modeling viscosity data.

Table: D.1: detailed calculation for modeling MEA viscosity data

T	M_MEA (kg/mol)	M_H2O (kg/mol)	x MEA	Density pure MEA	Density pure H2O	Viscosity of pure MEA (m.Pa.s)	Viscosity of pure water (m.Pa.s)	Molar volume of pure MEA (m^3)	Molar volume of pure H2O (m^3)	Measured Density of mixture Kg/m^3	M_MIX (Kg/mol)	Molar volume of mixture (m^3)	Measured viscosity of mixture (m.Pa.s)	ΔG^{E*} (J/mol)	ΔG^* (J/mol)	ΔG^{E*} (J/mol) correlation	V Ideal	Etha Ideal	etha calc
303.15	0.06108	0.01801528	0.112314466	1008.1	995.67	14.698	0.7960	6.05892E-05	1.81E-05	1008.260	0.0229	2.2665E-05	2.112333	7.38E-01	1.42E+03	7.13E-01	2.3E-05	2.4E+00	2.4E+00
313.15	0.06108	0.01801528	0.112314466	1000.1	999.99	9.9987	0.7180	6.10739E-05	1.80E-05	1003.770	0.0229	2.2766E-05	1.658567	6.38E-01	1.52E+03	9.53E-01	2.3E-05	1.8E+00	1.8E+00
323.15	0.06108	0.01801528	0.112314466	992.1	999.75	6.927	0.6520	6.15664E-05	1.80E-05	998.040	0.0229	2.2897E-05	1.316333	5.39E-01	1.63E+03	1.18E+00	2.3E-05	1.4E+00	1.4E+00
333.15	0.06108	0.01801528	0.112314466	984	999.07	5.049	0.5950	6.20732E-05	1.80E-05	992.230	0.0229	2.3031E-05	1.081733	4.63E-01	1.73E+03	1.35E+00	2.3E-05	1.1E+00	1.1E+00
343.15	0.06108	0.01801528	0.112314466	975.9	998.02	3.817	0.5470	6.25884E-05	1.81E-05	985.690	0.0229	2.3184E-05	0.906477	3.98E-01	1.82E+03	1.43E+00	2.3E-05	1.1E+00	9.1E-01
353.15	0.06108	0.01801528	0.112314466	967.6	996.69	2.963	1.0020	6.31253E-05	1.80E-05	976.560	0.0229	2.3401E-05	0.76128	-2.79E-01	1.92E+03	1.33E+00	2.5E-05	1.7E+00	1.2E+00
303.15	0.06108	0.01801528	0.16430408	1008.1	995.67	14.698	0.7960	6.05892E-05	1.81E-05	1013.420	0.0251	2.4759E-05	3.2547	1.04E+00	1.31E+03	8.92E-01	2.5E-05	3.1E+00	3.1E+00
313.15	0.06108	0.01801528	0.16430408	1000.1	999.99	9.9987	0.7180	6.10739E-05	1.80E-05	1007.830	0.0251	2.4896E-05	2.4674	1.04E+00	1.42E+03	1.42E+00	2.5E-05	2.3E+00	2.3E+00
323.15	0.06108	0.01801528	0.16430408	992.1	999.75	6.927	0.6520	6.15664E-05	1.80E-05	1001.910	0.0251	2.5043E-05	2.012633	8.66E-01	1.51E+03	1.42E+00	2.5E-05	1.7E+00	1.7E+00
333.15	0.06108	0.01801528	0.16430408	984	999.07	5.049	0.5950	6.20732E-05	1.80E-05	995.650	0.0251	2.5201E-05	1.80222	8.88E-01	1.58E+03	9.80E-01	2.5E-05	1.3E+00	1.3E+00
343.15	0.06108	0.01801528	0.16430408	975.9	998.02	3.817	0.5470	6.25884E-05	1.81E-05	989.000	0.0251	2.537E-05	1.5553	8.62E-01	1.67E+03	1.18E+00	2.5E-05	1.3E+00	1.3E+00
353.15	0.06108	0.01801528	0.16430408	967.6	996.69	2.963	1.0020	6.31253E-05	1.80E-05	982.020	0.0251	2.555E-05	1.2545	1.10E+00	1.77E+03	1.32E+00	2.5E-05	1.3E+00	1.3E+00
303.15	0.06108	0.01801528	0.227675393	1008.1	995.67	14.698	0.7960	6.05892E-05	1.81E-05	1018.110	0.0278	2.7325E-05	4.771233	1.26E+00	1.21E+03	1.36E+00	2.8E-05	4.0E+00	4.0E+00
313.15	0.06108	0.01801528	0.227675393	1000.1	999.99	9.9987	0.7180	6.10739E-05	1.80E-05	1011.810	0.0278	2.7495E-05	3.522133	1.14E+00	1.32E+03	1.24E+00	2.8E-05	2.8E+00	2.9E+00
323.15	0.06108	0.01801528	0.227675393	992.1	999.75	6.927	0.6520	6.15664E-05	1.80E-05	1005.730	0.0278	2.7662E-05	2.718233	1.04E+00	1.42E+03	8.54E-01	2.8E-05	2.1E+00	2.1E+00
333.15	0.06108	0.01801528	0.227675393	984	999.07	5.049	0.5950	6.20732E-05	1.80E-05	998.620	0.0278	2.7859E-05	1.99	8.74E-01	1.54E+03	7.00E-01	2.8E-05	1.6E+00	1.6E+00
343.15	0.06108	0.01801528	0.227675393	975.9	998.02	3.817	0.5470	6.25884E-05	1.81E-05	991.620	0.0278	2.8055E-05	1.571	7.71E-01	1.65E+03	9.10E-01	2.8E-05	1.3E+00	1.3E+00
353.15	0.06108	0.01801528	0.227675393	967.6	996.69	2.963	1.0020	6.31253E-05	1.80E-05	984.250	0.0278	2.8265E-05	1.2334	1.23E-01	1.76E+03	1.09E+00	2.8E-05	1.4E+00	1.5E+00
303.15	0.06108	0.01801528	0.306769532	1008.1	995.67	14.698	0.7960	6.05892E-05	1.81E-05	1021.370	0.0312	3.0573E-05	6.6926	1.39E+00	1.12E+03	1.21E+00	3.1E-05	5.1E+00	5.2E+00
313.15	0.06108	0.01801528	0.306769532	1000.1	999.99	9.9987	0.7180	6.10739E-05	1.80E-05	1014.640	0.0312	3.0776E-05	4.72725	1.24E+00	1.24E+03	1.24E+00	3.1E-05	3.6E+00	3.6E+00
323.15	0.06108	0.01801528	0.306769532	992.1	999.75	6.927	0.6520	6.15664E-05	1.80E-05	1007.730	0.0312	3.0987E-05	3.44265	1.10E+00	1.35E+03	1.12E+00	3.1E-05	2.6E+00	2.6E+00
333.15	0.06108	0.01801528	0.306769532	984	999.07	5.049	0.5950	6.20732E-05	1.80E-05	999.820	0.0312	3.1232E-05	2.56325	9.75E-01	1.47E+03	7.81E-01	3.2E-05	2.0E+00	2.0E+00
343.15	0.06108	0.01801528	0.306769532	975.9	998.02	3.817	0.5470	6.25884E-05	1.81E-05	992.520	0.0312	3.1462E-05	1.9861	8.68E-01	1.57E+03	5.66E-01	3.2E-05	1.6E+00	1.6E+00
353.15	0.06108	0.01801528	0.306769532	967.6	996.69	2.963	1.0020	6.31253E-05	1.80E-05	985.480	0.0312	3.1686E-05	1.5595	1.35E+00	1.68E+03	7.44E-01	3.2E-05	1.6E+00	1.6E+00
303.15	0.06108	0.01801528	0.40704578	1008.1	995.67	14.698	0.7960	6.05892E-05	1.81E-05	1022.700	0.0355	3.4756E-05	9.7273	1.48E+00	1.03E+03	8.99E-01	3.5E-05	6.5E+00	6.6E+00
313.15	0.06108	0.01801528	0.40704578	1000.1	999.99	9.9987	0.7180	6.10739E-05	1.80E-05	1015.470	0.0355	3.5003E-05	6.59515	1.31E+00	1.15E+03	1.01E+00	3.6E-05	4.5E+00	4.6E+00
323.15	0.06108	0.01801528	0.40704578	992.1	999.75	6.927	0.6520	6.15664E-05	1.80E-05	1008.120	0.0355	3.5258E-05	4.64905	1.17E+00	1.27E+03	1.05E+00	3.6E-05	3.2E+00	3.3E+00
333.15	0.06108	0.01801528	0.40704578	984	999.07	5.049	0.5950	6.20732E-05	1.80E-05	1000.600	0.0355	3.5523E-05	3.3967	1.05E+00	1.38E+03	9.66E-01	3.6E-05	2.4E+00	2.4E+00
343.15	0.06108	0.01801528	0.40704578	975.9	998.02	3.817	0.5470	6.25884E-05	1.81E-05	992.600	0.0355	3.581E-05	2.5793	9.39E-01	1.49E+03	6.74E-01	3.6E-05	1.9E+00	1.9E+00
353.15	0.06108	0.01801528	0.40704578	967.6	996.69	2.963	1.0020	6.31253E-05	1.80E-05	985.530	0.0355	3.6066E-05	1.99485	4.29E-01	1.60E+03	3.48E-01	3.6E-05	1.8E+00	1.8E+00
303.15	0.06108	0.01801528	0.541095919	1008.1	995.67	14.698	0.7960	6.05892E-05	1.81E-05	1020.990	0.0413	4.0468E-05	12.7985	1.35E+00	9.53E+02	4.80E-01	4.1E-05	8.3E+00	8.5E+00
313.15	0.06108	0.01801528	0.541095919	1000.1	999.99	9.9987	0.7180	6.10739E-05	1.80E-05	1013.470	0.0413	4.0768E-05	8.54765	1.21E+00	1.07E+03	6.14E-01	4.1E-05	5.7E+00	5.8E+00
323.15	0.06108	0.01801528	0.541095919	992.1	999.75	6.927	0.6520	6.15664E-05	1.80E-05	1005.870	0.0413	4.1076E-05	5.9739	1.10E+00	1.19E+03	7.34E-01	4.2E-05	4.0E+00	4.1E+00
333.15	0.06108	0.01801528	0.541095919	984	999.07	5.049	0.5950	6.20732E-05	1.80E-05	998.040	0.0413	4.1399E-05	4.2661	9.75E-01	1.31E+03	8.09E-01	4.2E-05	3.0E+00	3.0E+00
343.15	0.06108	0.01801528	0.541095919	975.9	998.02	3.817	0.5470	6.25884E-05	1.81E-05	990.180	0.0413	4.1727E-05	3.1675	8.70E-01	1.42E+03	7.78E-01	4.2E-05	2.3E+00	2.3E+00
353.15	0.06108	0.01801528	0.541095919	967.6	996.69	2.963	1.0020	6.31253E-05	1.80E-05	982.120	0.0413	4.207E-05	2.42215	4.64E-01	1.53E+03	5.32E-01	4.2E-05	2.1E+00	2.1E+00
303.15	0.06108	0.01801528	0.72599033	1008.1	995.67	14.698	0.7960	6.05892E-05	1.81E-05	1016.110	0.0493	4.8499E-05	14.898	8.24E-01	9.06E+02	4.53E-02	4.9E-05	1.1E+01	1.1E+01
313.15	0.06108	0.01801528	0.72599033	1000.1	999.99	9.9987	0.7180	6.10739E-05	1.80E-05	1008.430	0.0493	4.8868E-05	9.9105	7.49E-01	9.21E+02	1.21E-01	4.9E-05	7.5E+00	7.5E+00
323.15	0.06108	0.01801528	0.72599033	992.1	999.75	6.927	0.6520	6.15664E-05	1.80E-05	1000.420	0.0493	4.9259E-05	6.84495	6.72E-01	1.03E+03	2.32E-01	5.0E-05	5.2E+00	5.3E+00
333.15	0.06108	0.01801528	0.72599033	984	999.07	5.049	0.5950	6.20732E-05	1.80E-05	992.430	0.0493	4.9656E-05	4.9031	5.98E-01	1.14E+03	3.72E-01	5.0E-05	3.8E+00	3.9E+00
343.15	0.06108	0.01801528	0.72599033	975.9	998.02	3.817	0.5470	6.25884E-05	1.81E-05	984.450	0.0493	5.0058E-05	3.6252	3.41E-01	1.26E+03	5.07E-01	5.0E-05	2.9E+00	2.9E+00
353.15	0.06108	0.01801528	0.72599033	967.6	996.69	2.963	1.0020	6.31253E-05	1.80E-05	976.300	0.0493	5.0476E-05	2.74935	6.05E-04	1.37E+03	5.56E-01	5.1E-05	2.4E+00	2.4E+00
303.15	0.06108	0.01801528	1	1008.1	995.67	14.698	0.7960	6.05892E-05	1.81E-05	1008.710	0.0611	6.0553E-05	14.698	7.00E-05	8.92E+02	3.57E-01	6.1E-05	1.5E+01	1.5E+01
313.15	0.06108	0.01801528	1	1000.1	999.99	9.9987	0.7180	6.10739E-05	1.80E-05	1000.030	0.0611	6.1078E-05	9.9987	7.06E-05	1.00E+03	0.00E+00	6.2E-05	1.0E+01	1.0E+01
323.15	0.06108	0.01801528	1	992.1	999.75	6.927	0.6520	6.15664E-05	1.80E-05	992.030	0.0611	6.1571E-05	6.927	4.07E-05	1.12E+03	0.00E+00	6.2E-05	6.9E+00	6.9E+00
333.15	0.06108	0.01801528	1	984	999.07	5.049	0.5950	6.20732E-05	1.80E-05	983.960	0.0611	6.2076E-05	5.049	-1.02E-05	1.23E+03	0.00E+00	6.3E-05	5.0E+00	5.1E+00
343.15	0.06108	0.01801528	1	975.9	998.02	3.817	0.5470	6.25884E-05	1.81E-05	975.910	0.0611	6.2588E-05	3.817	-7.23E-05	1.33E+03	0.00E+00	6.3E-05	3.8E+00	3.8E+00
353.15	0.06108	0.01801528	1	967.6	996.69	2.963	1.0020	6.31253E-05	1.81E-05	967.670	0.0611	6.3121E-05	2.963	0.00E+00	1.43E+03	0.00E+00	6.3E-05	3.0E+00	3.0E+00

Table: D.2: detailed calculation for modeling MEA viscosity data

T	T(C)	w	M_AMP (kg/m³)	M_H2O (kg/m³)	x AMP	x H2O	Density pure AMP	Density of pure H2O	Viscosity of pure AMP (m.Pa.s)	Viscosity of pure water (m.Pa.s)	Molar volume of pure MEA (m³)	Molar volume (m³)	Measured Density of mixture kg/m³	M_MIX (kg/mol)	Molar volume of mixture (m³)	Measured viscosity of mixture (m.Pa.s)	ΔG^{E*} J/mol	ΔG^* J/mol	DeltaGE/RT model
313.15	40	30	0.3472212	0.01801528	0.0797	0.920281	919.75	999.99	47.8	0.718	0.000377517	1.80151E-05	988.58	0.04259247	4.47705E-05	2.1748	3752.521349	1372.698411	-2.47E+03
323.15	50	30	0.3472212	0.01801528	0.0797	0.920281	910.27	999.75	25.1	0.652	0.000381449	1.80198E-05	982.15	0.04259247	4.50636E-05	1.6306	3489.716683	1482.241918	-2.89E+03
333.15	60	30	0.3472212	0.01801528	0.0797	0.920281	901.62	999.07	14.4	0.595	0.000385108	1.8032E-05	974.95	0.04259247	4.53964E-05	1.253	3240.536008	1589.813816	-2.92E+03
343.15	70	30	0.3472212	0.01801528	0.0797	0.920281	892.92	998.02	8.91	0.547	0.00038886	1.80516E-05	963.13	0.04259247	4.59536E-05	0.99011	3025.84663	1693.466536	-2.41E+03
353.15	80	30	0.3472212	0.01801528	0.0797	0.920281	884.07	996.69	5.808247495	1.002	0.000392753	1.80751E-05	947.82	0.04259247	4.66958E-05	0.79792	986.1121469	1794.719268	-1.32E+03
313.15	40	40	0.3472212	0.01801528	0.1187	0.881297	919.75	999.99	47.8	0.718	0.000377517	1.80155E-05	985.97	0.05709048	5.79055E-05	3.338133333	4802.953191	1249.126245	-1.21E+02
323.15	50	40	0.3472212	0.01801528	0.1187	0.881297	910.27	999.75	25.1	0.652	0.000381449	1.80198E-05	978.69	0.05709048	5.83362E-05	2.4043	4524.471423	1362.344846	-8.88E+02
333.15	60	40	0.3472212	0.01801528	0.1187	0.881297	901.62	999.07	14.4	0.595	0.000385108	1.8032E-05	971.13	0.05709048	5.87903E-05	1.761033333	4224.757741	1476.055982	-2.49E+03
343.15	70	40	0.3472212	0.01801528	0.1187	0.881297	892.92	998.02	8.91	0.547	0.00038886	1.80516E-05	963.3	0.05709048	5.92682E-05	1.336633333	3956.103292	1585.389584	-2.46E+03
353.15	80	40	0.3472212	0.01801528	0.1187	0.881297	884.07	996.69	5.808247495	1.002	0.000392753	1.80751E-05	954.3	0.05709048	5.98271E-05	1.039666667	1937.191716	1692.204225	-2.88E+03
313.15	40	50	0.3472212	0.01801528	0.1683	0.831706	919.75	999.99	47.8	0.718	0.000377517	1.80151E-05	981.2	0.073418699	7.48254E-05	5.36785	5772.216397	1120.89586	-2.92E+03
323.15	50	50	0.3472212	0.01801528	0.1683	0.831706	910.27	999.75	25.1	0.652	0.000381449	1.80198E-05	973.33	0.073418699	7.54304E-05	3.70115	5480.818646	1238.136271	-2.41E+03
333.15	60	50	0.3472212	0.01801528	0.1683	0.831706	901.62	999.07	14.4	0.595	0.000385108	1.8032E-05	965.25	0.073418699	7.60618E-05	2.6611	5223.478572	1350.733592	-1.32E+03
343.15	70	50	0.3472212	0.01801528	0.1683	0.831706	892.92	998.02	8.91	0.547	0.00038886	1.80516E-05	956.96	0.073418699	7.67208E-05	2.00665	5022.49072	1456.481567	-1.21E+02
353.15	80	50	0.3472212	0.01801528	0.1683	0.831706	884.07	996.69	5.808247495	1.002	0.000392753	1.80751E-05	948.11	0.073418699	7.74369E-05	1.56055	3183.043651	1558.411354	-8.88E+02
313.15	40	60	0.3472212	0.01801528	0.2326	0.767434	919.75	999.99	47.8	0.718	0.000377517	1.80151E-05	974.0	0.094577269	9.71009E-05	8.54925	6450.796772	999.641587	-2.49E+03
323.15	50	60	0.3472212	0.01801528	0.2326	0.767434	910.27	999.75	25.1	0.652	0.000381449	1.80198E-05	965.85	0.094577269	9.79213E-05	5.607	6140.417035	1122.182219	-2.46E+03
333.15	60	60	0.3472212	0.01801528	0.2326	0.767434	901.62	999.07	14.4	0.595	0.000385108	1.8032E-05	957.53	0.094577269	9.87721E-05	3.8805	5880.143095	1238.155739	-2.88E+03
343.15	70	60	0.3472212	0.01801528	0.2326	0.767434	892.92	998.02	8.91	0.547	0.00038886	1.80516E-05	948.97	0.094577269	9.96631E-05	2.80105	5645.823981	1349.259327	-2.91E+03
353.15	80	60	0.3472212	0.01801528	0.2326	0.767434	884.07	996.69	5.808247495	1.002	0.000392753	1.80751E-05	940.21	0.094577269	0.000100592	2.08975	3895.924608	1456.699482	-2.41E+03
313.15	40	70	0.3472212	0.01801528	0.3205	0.679458	919.75	999.99	47.8	0.718	0.000377517	1.80151E-05	964.46	0.12353957	0.000128092	14.029	6802.979571	876.1022596	-1.31E+03
323.15	50	70	0.3472212	0.01801528	0.3205	0.679458	910.27	999.75	25.1	0.652	0.000381449	1.80198E-05	956.24	0.12353957	0.000129193	8.7953	6510.192528	1002.33862	-1.21E+02
333.15	60	70	0.3472212	0.01801528	0.3205	0.679458	901.62	999.07	14.4	0.595	0.000385108	1.8032E-05	947.83	0.12353957	0.000130339	5.81505	6245.791924	1122.902328	-8.88E+02
343.15	70	70	0.3472212	0.01801528	0.3205	0.679458	892.92	998.02	8.91	0.547	0.00038886	1.80516E-05	939.21	0.12353957	0.000131536	4.0435	6013.788679	1237.3687	-2.49E+03
353.15	80	70	0.3472212	0.01801528	0.3205	0.679458	884.07	996.69	5.808247495	1.002	0.000392753	1.80751E-05	930.35	0.12353957	0.000132788	2.94505	4469.405824	1345.66539	-2.45E+03
313.15	40	80	0.3472212	0.01801528	0.4470	0.553044	919.75	999.99	47.8	0.718	0.000377517	1.80155E-05	952.41	0.165155933	0.000173408	23.559	6558.129201	751.7009019	-2.87E+03
323.15	50	80	0.3472212	0.01801528	0.4470	0.553044	910.27	999.75	25.1	0.652	0.000381449	1.80198E-05	944.12	0.165155933	0.000174931	13.9095	6279.333839	884.1601592	-2.90E+03
333.15	60	80	0.3472212	0.01801528	0.4470	0.553044	901.62	999.07	14.4	0.595	0.000385108	1.8032E-05	935.63	0.165155933	0.000176518	8.69985	6014.038711	1010.871177	-2.40E+03
343.15	70	80	0.3472212	0.01801528	0.4470	0.553044	892.92	998.02	8.91	0.547	0.00038886	1.80516E-05	926.93	0.165155933	0.000178175	5.75035	5770.79	1131.267122	-1.31E+03
353.15	80	80	0.3472212	0.01801528	0.4470	0.553044	884.07	996.69	5.808247495	1.002	0.000392753	1.80751E-05	918.05	0.165155933	0.000179899	3.97165	4444.046173	1246.835785	-1.21E+02
313.15	40	90	0.3472212	0.01801528	0.6449	0.355093	919.75	999.99	47.8	0.718	0.000377517	1.80155E-05	937.71	0.230322347	0.000245622	31.1765	4462.296662	677.3515329	-8.87E+02
323.15	50	90	0.3472212	0.01801528	0.6449	0.355093	910.27	999.75	25.1	0.652	0.000381449	1.80198E-05	929.38	0.230322347	0.000247824	17.9665	4337.905311	809.524521	-2.45E+03
333.15	60	90	0.3472212	0.01801528	0.6449	0.355093	901.62	999.07	14.4	0.595	0.000385108	1.8032E-05	920.99	0.230322347	0.000250081	10.9705	4195.691407	936.3687272	-2.87E+03
343.15	70	90	0.3472212	0.01801528	0.6449	0.355093	892.92	998.02	8.91	0.547	0.00038886	1.80516E-05	912.3	0.230322347	0.000252463	7.0823	4049.746645	1057.255849	-2.90E+03
353.15	80	90	0.3472212	0.01801528	0.6449	0.355093	884.07	996.69	5.808247495	1.002	0.000392753	1.80751E-05	903.42	0.230322347	0.000254945	4.79305	3209.028132	1173.025818	-2.40E+03
313.15	40	95	0.3472212	0.01801528	0.7797	0.220269	919.75	999.99	47.8	0.718	0.000377517	1.80155E-05	929.6	0.274707341	0.000295511	46.448	3440.044372	591.285644	-2.40E+03
323.15	50	95	0.3472212	0.01801528	0.7797	0.220269	910.27	999.75	25.1	0.652	0.000381449	1.80198E-05	921.21	0.274707341	0.000298203	25.067	3301.818488	732.285267	-1.31E+03
333.15	60	95	0.3472212	0.01801528	0.7797	0.220269	901.62	999.07	14.4	0.595	0.000385108	1.8032E-05	912.65	0.274707341	0.000301	14.4795	3144.526298	866.7478711	-1.22E+02
343.15	70	95	0.3472212	0.01801528	0.7797	0.220269	892.92	998.02	8.91	0.547	0.00038886	1.80516E-05	903.85	0.274707341	0.000300393	8.95555	2994.350587	993.3370213	-8.87E+02
353.15	80	95	0.3472212	0.01801528	0.7797	0.220269	884.07	996.69	5.808247495	1.002	0.000392753	1.80751E-05	894.99	0.274707341	0.000306699	5.85685	2428.162211	1113.538432	-2.49E+03

Sample MATLAB code used to fit MEA viscosity data to Eyring's viscosity model

```
function [fitresult, gof] = createFit(x_MEA_V, T_MEA_V, DltaGE_MEA)
%CREATEFIT(X_MEA_V,T_MEA_V,DLTAGE_MEA)
%  Create a fit.
%
%  Data for 'untitled fit 1' fit:
%      X Input: x_MEA_V
%      Y Input: T_MEA_V
%      Z Output: DltaGE_MEA
%  Output:
%      fitresult : a fit object representing the fit.
%      gof : structure with goodness-of fit info.
%
%  See also FIT, CFIT, SFIT.

%  Auto-generated by MATLAB on 30-Apr-2023 16:07:48


%% Fit: 'untitled fit 1'.
[xData, yData, zData] = prepareSurfaceData( x_MEA_V, T_MEA_V, DltaGE_MEA );

% Set up fittype and options.
ft = fittype( 'x_MEA_V*(1-
x_MEA_V)*((a0+b0*T_MEA_V+c0*T_MEA_V^2)+((a1+b1*T_MEA_V+c1*T_MEA_V^2)*(1-2*(1-
x_MEA_V)))+((a2+b2*T_MEA_V+c2*T_MEA_V^2)*((1-2*(1-
x_MEA_V))^2))+((a3+b3*T_MEA_V+c3*T_MEA_V^2)*((1-2*(1-x_MEA_V))^3)))', 'independent',
{'x_MEA_V', 'T_MEA_V'}, 'dependent', 'z' );
opts = fitoptions( 'Method', 'NonlinearLeastSquares' );
opts.Display = 'Off';
opts.StartPoint = [0.152378018969223 0.825816977489547 0.538342435260057
0.9961347166626885 0.0781755287531837 0.442678269775446 0.106652770180584
0.961898080855054 0.00463422413406744 0.774910464711502 0.817303220653433
0.86869470536351];

% Fit model to data.
[fitresult, gof] = fit( [xData, yData], zData, ft, opts );

% Plot fit with data.
figure( 'Name', 'untitled fit 1' );
h = plot( fitresult, [xData, yData], zData );
legend( h, 'untitled fit 1', 'DltaGE_MEA vs. x_MEA_V, T_MEA_V', 'Location',
'NorthEast', 'Interpreter', 'none' );
% Label axes
xlabel( 'x_MEA_V', 'Interpreter', 'none' );
ylabel( 'T_MEA_V', 'Interpreter', 'none' );
zlabel( 'DltaGE_MEA', 'Interpreter', 'none' );
grid on
```

Sample MATLAB code used to fit AMP viscosity data to Arrhenius equation

```matlab
function [fitresult, gof] = createFit(x_AMP_AR, T_AMP_AR, RH_AMP)
%CREATEFIT(X_AMP_AR,T_AMP_AR,RH_AMP)
%  Create a fit.
%
%  Data for 'untitled fit 1' fit:
%      X Input: x_AMP_AR
%      Y Input: T_AMP_AR
%      Z Output: RH_AMP
%  Output:
%      fitresult : a fit object representing the fit.
%      gof : structure with goodness-of fit info.
%
%  See also FIT, CFIT, SFIT.

%  Auto-generated by MATLAB on 30-Apr-2023 16:09:48


%% Fit: 'untitled fit 1'.
[xData, yData, zData] = prepareSurfaceData( x_AMP_AR, T_AMP_AR, RH_AMP );

% Set up fittype and options.
ft = fittype( '(k1+((k2*(1-
x_AMP_AR))/T_AMP_AR))*exp((k3/T_AMP_AR)+(k4*x_AMP_AR/T_AMP_AR)+(k5*((x_AMP_AR/T_AMP_A
R)^2)))', 'independent', {'x_AMP_AR', 'T_AMP_AR'}, 'dependent', 'z' );
opts = fitoptions( 'Method', 'NonlinearLeastSquares' );
opts.Display = 'Off';
opts.StartPoint = [0.706046088019609 0.0318328463774207 0.27692298496089
0.0461713906311539 0.0971317812358475];

% Fit model to data.
[fitresult, gof] = fit( [xData, yData], zData, ft, opts );

% Plot fit with data.
figure( 'Name', 'untitled fit 1' );
h = plot( fitresult, [xData, yData], zData );
legend( h, 'untitled fit 1', 'RH_AMP vs. x_AMP_AR, T_AMP_AR', 'Location',
'NorthEast', 'Interpreter', 'none' );
% Label axes
xlabel( 'x_AMP_AR', 'Interpreter', 'none' );
ylabel( 'T_AMP_AR', 'Interpreter', 'none' );
zlabel( 'RH_AMP', 'Interpreter', 'none' );
grid on
```